THE THEORY OF THE SOUND FIELD NEAR A CAUSTIC

M. J. Daintith

Admiralty Underwater Weapons Establishment

Prepared for:

Defence Scientific Information Centre

May 1973

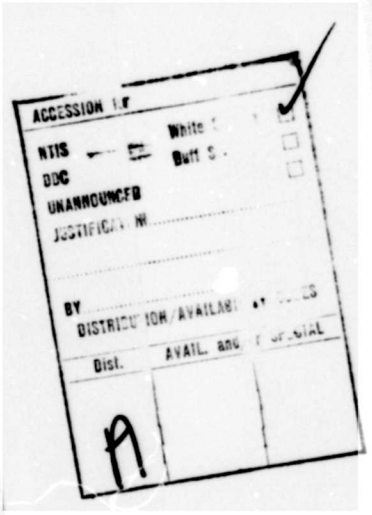

The views expressed herein do not necessarily represent the considered opinion of the issuing establishment and must not be taken to define Ministry of Defence (Naval) or Departmental policy.

AMENDMENTS

NUMBER	1	2	3	4	5	6	7	8	9	10
DATE										

UNCLASSIFIED UNLIMITED

AD787831

U.K. ABSTRACT NO.

(A)	Country of Origin	UNITED KINGDOM
(B)	Establishment of Origin with Short Address	Admiralty Underwater Weapons Establishment, Portland.
(C)	Title of Report	The Theory of the Sound Field near a Caustic
(D)	Author	M.J. Daintith
(E)	Pages and Figures	32 pages ((i) - (ii) (1 - 30)) Figs. 12
(F)	Date	May, 1973
(G)	Originator's Reference	Technical Note 485/73 - BR 41213
(H)	Security Grading	UNCLASSIFIED UNLIMITED
(J)	Abstract	Impulse analysis of the wave equation leads to a convenient approximation for the intensity over a caustic, the field being an interference pattern between two rays. The result, which holds over much of the sonar frequency band, involves only a simple addition to conventional ray-tracing computations. A critical experiment test of the theory is proposed.

U.D.C. No. 534.6:
534.231:
534.21

A.U.W.E. Technical Note 485/73
May, 1973

THE THEORY OF THE SOUND FIELD NEAR A CAUSTIC

by

M. J. Daintith

CONTENTS

ILLUSTRATIONS

Figure

THE THEORY OF THE SOUND FIELD NEAR A CAUSTIC

PRÉCIS

1. The linear wave equation has an exact solution in terms of impulse functions. The resulting expressions bear a strong resemblance to those used in 'geometric' acoustics, and are computed from conventional ray tracing techniques, but involve certain constants which may be used to generate the solution in situations where geometric acoustics break down, such as convergence and shadow zones. From these 'impulse' solutions the pressure field from a point source of any form is given by a simple convolution.

2. This theory, applied to a convergence zone, shows that the field near a convergence zone is essentially an interference pattern formed by two nearly coincident 'rays'; at the caustic itself the two rays coalesce, following identical paths, and must therefore be added coherently. One of these rays has been tangential to the caustic at an earlier point in its path; from the physical condition that the intensity remains finite at the caustic, it is shown that the contribution from this ray is to be computed as if it were phase-inverted on passing the caustic. As a result, although the intensity for either component ray tends to infinity at the caustic, the resultant is well-behaved. The caustic itself is, in fact, a region of low intensity, a peak value occurring some distance away.

3. The interference pattern, at sonar frequencies, is closely spaced, the interference fringes being parallel to the caustic itself. There is a focussing zone, extending, at sonar frequencies, only a few hundred metres from the caustic. The mean intensity in this zone falls off from the peak as the square root of the distance from the caustic. The 'fine structure' about the mean level is dominated by the form of source signal.

4. The analysis leads naturally to a useful approximation holding over the focussing region of the convergence zone. For a stratified medium the only computed parameter other than those computed in a normal ray-tracing programme is the curvature of the range/initial grazing angle plot.

5. The approximate expression for the pressure field is:-

$$p = \frac{\text{Cot } \theta_o}{x\sqrt{2yr}} \left[S_o (T + \Delta) - S_o (T - \Delta) \right]$$

where $$\Delta = \frac{\text{Sin } \alpha_o \, (2r)^{3/2}}{3C_s \, y^{\frac{1}{2}}}$$

$$T = t - \tau_o - r \text{ Cos } \alpha_o / C_s$$

Subscript $_o$ refers to a point on the caustic at the same depth as the field point - termed the 'caustic point' in the following definitions:

$S_o(t)$ is the time-variance of the source point

p is pressure at the field point

α_o is the initial grazing angle of the ray passing through the caustic point

C_s is sound speed at source

r is horizontal range from caustic to field points

x is horizontal range from source to caustic point

t is time

τ_o is travel time along range to the caustic point

γ is the curvature of the (x,α) plot at the caustic point, i.e. it is

$$\left(\frac{\partial^2 x}{\partial \alpha^2}\right)_o$$

This expression holds for sonar frequencies from a few hundred Hertz upwards.

CONCLUSIONS AND RECOMMENDATIONS

6. The theory presented here gives a simple and plausible account of the structure of the field near a caustic, based upon a valid solution of the wave equation.

7. The phenomenon is essentially one of coherent interference between two rays, one computed normally, the other, which has already touched the caustic, being phase-inverted.

8. A simple and practical transition formula for the field, requiring little extra computation beyond that used for conventional ray-tracing, gives results which are similar to those observed in practice.

9. The field at the caustic itself is very small. The peak of the focussing region occurs at a short distance beyond the caustic (typically 100 m).

10. For band-limited signals there is an inherent fine structure, of spacing typically a few tens of metres horizontally, and a few metres vertically. It is suggested that this, and not complexities in sound speed profile, is the major source of field structure near the caustic.

11. The 'impulse technique' on which the study is based is simple to understand in physical terms, is easy to apply to complex signals, and involves only simple mathematical functions.

12. The result is an extremely general one, its form being independent of the detailed structure of the medium and the method of formation of the caustic.

13. The method is essentially a 'high-frequency' solution, and therefore complements Fourier-type analyses which are biassed to low frequencies. Over much of the frequency band of interest in the sonar world the impulse solution is valid.

14. It is recommended that a crucial experimental test of the theory be made, using a vertical string of hydrophones to study the depth-dependent fine structure of the field near a convergence zone.

INTRODUCTION

15. The computation of the acoustic sound field in the vicinity of a caustic is commonly quoted as an example of the failure of 'ray acoustics', since this technique appears to predict infinite intensities at the Caustic itself. To date, the only satisfactory theoretical treatment has involved finding sinusoidal solutions of the wave equation for particular specifications of the sound speed profile, leading typically to Airy-functions. Recent developments in these methods have concentrated on a modified ray theory, 'rays' here being in essence defined as the normals to surfaces of constant phase. The modified rays are not coincident with the rays of geometric acoustics (although they are nearly so over a wide band of frequencies of interest), but in the neighbourhood of a caustic they have some disconcerting properties, which make them physically difficult to interpret, and introduce computational complexities.

16. The analysis in this paper sets out a different approach to the solution of the wave equation, that is, the use of the elementary solution for an impulse source. It will be shown that this method enables us to retain the rays of geometric acoustics and to produce a useful transition function which holds right up to the caustic, for a rather generally specified sound speed profile. It also gives the solution in a form which is readily calculable.

17. For convenience, a resumé of the principal features of the impulse solution prefaces the main analyis.

THE IMPULSE SOLUTION

18. In the impulse technique the solution of the linear wave equation $\nabla^2\phi = \frac{1}{C^2}\frac{\partial^2\phi}{\partial t^2}$, where ϕ is velocity potential, C the sound speed at the field point, and t is time, is found for an elementary source function H(t), where H is the Heaviside unit function (zero for $t < 0$, unity for $t > 0$).

19. It can be shown that, using this technique, the general solution for an arbitrary pressure source function $S_o(t)$ is given in the following way.

20. The solution is closely linked to the Huyghens wave fronts, that is, surfaces for which the travel time τ from the source, as defined by conventional ray tracing, is constant. Such surfaces always exist and are computable in principle everywhere in the field (even, for example, in shadow zones). From them rays may be defined as the orthogonal family of curves, and these, similarly, always exist. These rays are identical with those of conventional geometric acoustics (where the latter can be drawn).

21. The wavefronts move according to Huyghen's Principle, that is, orthogonally to themselves at the local sound speed C. In terms of travel time τ along a ray, this is equivalent to saying that the vector grad τ, which is normal to the wave-surface, has magnitude $\frac{1}{C}$. $\left|\text{Grad } \tau\right| = \nabla\tau = \frac{1}{C}$ is the general form of Snell's Law.

22. It should be noted that these results are derived from the linear wave equation, and are exact. They (and the results to follow, except where otherwise specified) are true for any acoustic field in a medium of any kind, provided only that we may assume the linear form of the wave equation to hold. They are valid, for example, even if the sound speed varies irregularly, or if it has discontinuities.

23. It can be deduced that the pressure field from a point source $S_o(t)$ is given at any point by an expression of the form

$$p = p_t + p_d$$

where p_t is termed the transport field and p_d the dispersive field. We consider each of these separately.

Transport Field

24. The transport field $p_t = S_o(t - \tau) \cdot A_o(\bar{x})$. $S_o(t - \tau)$ is a time-retarded replica of the source function and A_o is a function of the spatial coordinates only. It is the equivalent of the spherical spreading term $\frac{1}{R}$ for a point source in a uniform medium, and can be expressed in a form closely related to the 'geometric intensity' function of ray acoustics.

25. If we consider a ray tube emanating from the source, at which it subtends solid angle $d\Omega$, and if $d\sigma$ is the normal cross-sectional area of the ray tube at the field point, then

$$A_o = K \cdot \rho \sqrt{\left| \frac{C}{\left(\frac{\partial \sigma}{d\Omega}\right)} \right|}$$

where ρ and C are density and sound speed at the field point and K is a constant for a given ray. The term $\frac{\partial \sigma}{d\Omega}$, is, of course, the ratio used in conventional 'ray-tracing'.

26. The factor K needs explanation. It is introduced because this is a general solution, which will apply anywhere in the field, even if there is a discontinuity or singularity of some kind. There may be, for example, a discontinuity in ρ or C (in extreme cases this may be a rigid boundary); or the term $\frac{\partial \sigma}{\partial \Omega}$ may 'blow up'. Two examples of the latter are that $\frac{\partial \sigma}{\partial \Omega}$ may pass through zero, when A_o becomes infinite at the singular point or surface, or $\frac{\partial \sigma}{\partial \Omega}$ may diverge to infinity, when A_o will become zero. The first of these defines a caustic - the situation to be studied. The second defines the point of entry into a shadow zone. When passing through such a singularity it is necessary to adopt the generalised form for A_o in the new spatial domain, and to determine the appropriate value of K by applying the standard boundary conditions for pressure and normal particle velocity.

27. Provided, however, that the wave front has not passed through such a singularity between source and field point, the value of K for a point source is determinate as $\frac{1}{(\rho_s \sqrt{C_s})}$, where ρ_s and C_s are the values of ρ and C at the source. This will hold even if ρ and C have discontinuities in gradient or in higher derivatives; only a discontinuous change in magnitude will require us to adopt a new value of K.

28. The computation of the transport field therefore follows exactly the lines of conventional ray acoustics, and the result will differ numerically only by the factor $\frac{\rho}{\rho_s}\sqrt{\frac{C}{C_s}}$, which for practical situations in the sea is not significant (a fraction of 1 dB at most).

Dispersive Field

29. The dispersive field p_d is given by the convolution integral

$$p_d = \rho \int_\tau^\infty S_o(t-\theta)\,\frac{\partial A}{\partial \theta}(\bar{x},\theta)\,d\theta$$ where $a(\bar{x},\theta)$ is a solution of the equation $\nabla^2 a = \frac{1}{C^2}\frac{\partial^2 a}{\partial \theta^2}$. This contains a number of constants of integration which are determinable for a point source and can be used to carry the solution across singularities. It can be shown that this field originates from multiple scattering by the variations in the medium; it represents what happens behind the wave-front for an impulse source, whereas the transport field represents what happens at the wave-front itself.

30. For a CW source, $\exp(i\omega t)$, the dispersive field has an asymptotic expansion of the form

$$p_d = \left[\frac{A_1}{i\omega} + \frac{A_2}{i^2\omega^2} + \frac{A_3}{i^3\omega^3} + \cdots\right] \exp(i\omega t)\ ,$$

showing that p_t is, as might be expected, the high-frequency limiting field. It can be shown that p_d will be significant as compared to p_t only at great ranges and low frequencies, or in and near a shadow zone (in which p_t is zero). For the convergence zone situations with which we shall be dealing the dominant contribution will arise from p_t.

Stratified Medium

31. For a horizontally stratified medium the sound speed C is a function of the depth z only, and is independent of the horizontal range x. It is well known that in such a medium the result $|\nabla\tau| = \frac{1}{C}$ reduces to Snell's Law, $\cos\theta/C$ = constant along the ray = $\cos\alpha/C_s$, where θ is the grazing angle at the field point, α the initial grazing angle, and C_s the sound speed at the source.

32. We shall assume that the density is everywhere constant. In this case the transport field is easily shown to be

$$p_t = S_o(t-\tau)\cdot K(\alpha)\sqrt{\left|\frac{\cot\theta}{x\left(\frac{\partial x}{\partial \alpha}\right)_z}\right|} \qquad \ldots (1)$$

where $K(\alpha)$, the undetermined constant, is a function of initial grazing angle only, and equals unity for a ray which has not passed through a singularity; this ray will be termed a direct ray.

33. It is convenient at this point to deduce relationships between τ, the travel time along a ray, x, the horizontal range, and z, the depth.

34. We have the analytical relationship

$$\left(\frac{\partial\tau}{\partial\alpha}\right)_z = \left(\frac{\partial\tau}{\partial x}\right)_z \cdot \left(\frac{\partial x}{\partial\alpha}\right)_z$$

But $\left(\frac{\partial\tau}{\partial x}\right)_z$ is the x-component of the vector $\overline{\text{grad } \tau}$, which we know to have magnitude $\frac{1}{C}$ and to be in the direction θ with respect to the x-axis. It follows that $\left(\frac{\partial\tau}{\partial x}\right)_z = \frac{\cos\theta}{C} = \frac{\cos\alpha}{C_s}$, by Snell's Law. Hence, at every point in the field,

$$\left(\frac{\partial\tau}{\partial\alpha}\right)_z = \frac{\cos\alpha}{C_s}\left(\frac{\partial x}{\partial\alpha}\right)_z \quad . \qquad \ldots (2)$$

Similarly, it can be shown that

$$\left(\frac{\partial\tau}{\partial\alpha}\right)_x = \frac{\sin\theta}{C}\left(\frac{\partial z}{\partial\alpha}\right)_x \quad . \qquad \ldots (3)$$

THE FIELD NEAR A CAUSTIC IN A STRATIFIED MEDIUM

35. For convenience the analysis will be carried out with reference to a conventional first convergence zone. It will be seen, however, that the result is a general one which will apply to a large class of caustics, such as multiple convergence zones or from a deep source.

36. Figure 1 shows the normal ray representation of a convergence zone. Rays refracted upwards at a depth below the sound speed minimum cross rays which have been refracted at still greater depths. The envelope of these crossings generates a caustic surface, characterised by the property that all rays in a pencil lie on one side of the caustic only. If we fix attention on a particular depth there is a limiting ray of minimum horizontal range, as shown in Figure 2. This limiting ray is tangential to the caustic. Rays launched at initial grazing angles either greater or less than that of the limiting ray reach the given depth at a range greater than the minimum.

37. The caustic is thus defined, at a particular depth, by the equation $\left(\frac{\partial x}{\partial\alpha}\right)_z = 0$, where α is the initial grazing angle. This implies that, on the caustic, the value of the transport field p_t is apparently infinite (equation 1). This is physically unacceptable, and is often held to indicate that 'ray theory' fails near a caustic.

38. The resolution of this difficulty is apparent once it is realised that a 'ray' at the caustic is not a single ray, but two coincident rays; and that in the vicinity of the caustic there are two rays which have traversed nearly identical paths. We are dealing, in fact, with an interference pattern.

39. The situation can be clearly visualised by considering not rays, but wavefronts. Figure 3 shows a selection of progressive wavefronts. Because of the positive sound-speed gradient at depth the lower part of the wavefront overtakes the upper, forming a loop with a pair of cusps, as shown. The cusps trace out a pair of caustics. The full development of this wavefront will occur only if there are no boundaries to the medium; in a real ocean the sea surface and the sea bed will modify the wavefront picture, and either or both of the cusps may be suppressed. This does not affect the analysis; in which it is postulated that a caustic is found.

40. The crux of the argument is that near the caustic the wavefronts and the associated ray paths are almost coincident, and thus in this region the pressure fields associated with each of the contributary rays must be added coherently. The succeeding analysis demonstrates that this not only resolves the difficulty of the breakdown of 'ray acoustics', but in the process yields a useful approximation for the field near the caustic.

The Taylor Series Approximation

41. Since $(\frac{\partial x}{\partial \alpha})_z = 0$ at the caustic, a Taylor series expansion about the caustic along the line z = constant suggests itself. Figure 4 shows the essential elements in the expansion. At the caustic the range is x_o, and the limiting ray has grazing angle θ_o, an initial launching angle α_o, and travel time τ_o. At a short distance r in the x-direction from the caustic there are two rays. For each of these rays $x = x_o + r$. One of these rays, in this instance the one of greater launching angle α, greater grazing angle θ, and shorter travel time τ, is a 'direct' ray as previously defined; the other ray, whose parameters will be denoted by primes (θ', α' and τ') is one which has already passed through the caustic; it will be termed the 'caustic' ray. For the convergence zone under discussion the relations $\theta > \theta_o > \theta'$ and $\alpha > \alpha_o > \alpha'$ hold; this is not necessarily the case for other types of caustic, but it will always be true that α_o lies between α and α'.

42. As we desire an expansion about the caustic we shall write $\alpha = \alpha_o + \varepsilon$, $\alpha' = \alpha_o + \varepsilon'$, etc. It is clear that ε and ε' will have different signs. The quantities r, ε, and ε' are shown in Figure 2.

43. It is now straightforward to write down expressions for the transport pressures arising from the direct ray (p_t) and from the ray which has already passed through the caustic (p_t'). By the arguments of Section II, we may use equation (1) to give

$$\left.\begin{aligned} p_t &= S_o(t-\tau)\sqrt{\left|\frac{\cot\theta}{x(\frac{\partial x}{\partial \alpha})_z}\right|} \\ p_t' &= S_o(t-\tau')\,K(\alpha')\sqrt{\left|\frac{\cot\theta'}{x(\frac{\partial x}{\partial \alpha})_z'}\right|} \end{aligned}\right\} \quad \ldots (4)$$

44. A Taylor series expansion of x in terms of α about the point on the caustic yields immediately

$$x - x_o = r = \tfrac{1}{2}\varepsilon^2 \left[\left(\frac{\partial^2 x}{\partial \alpha^2}\right)_z\right]_o + \frac{\varepsilon^3}{6} \left[\left(\frac{\partial^3 x}{\partial \alpha^3}\right)_z\right]_o + \ldots \quad .$$

Writing $\left[\left(\frac{\partial^2 x}{\partial \alpha^2}\right)_z\right]_o = \gamma$ and $\left[\left(\frac{\partial^3 x}{\partial \alpha^3}\right)_z\right]_o = \beta$ the following equations follow immediately.

$$r = \tfrac{1}{2}\gamma\varepsilon^2 + \frac{1}{6}\beta\varepsilon^3 + O(\varepsilon^4) \qquad \ldots (5)$$

$$\left(\frac{\partial x}{\partial \alpha}\right)_z = \left(\frac{\partial r}{\partial \varepsilon}\right)_z = \gamma\varepsilon + \tfrac{1}{2}\beta\varepsilon^2 + O(\varepsilon^3) \quad . \qquad \ldots (6)$$

45. We may also find an expansion for travel time τ, by the use of equation (2). Successive differentiation with respect to α, keeping z constant, yields

$$\left(\frac{\partial \tau}{\partial \alpha}\right)_z = \frac{\cos \alpha}{C_s} \left(\frac{\partial x}{\partial \alpha}\right)_z$$

$$\left(\frac{\partial^2 \tau}{\partial \alpha^2}\right)_z = -\frac{\sin \alpha}{C_s} \left(\frac{\partial x}{\partial \alpha}\right)_z + \frac{\cos \alpha}{C_s} \left(\frac{\partial^2 x}{\partial \alpha^2}\right)_z$$

$$\left(\frac{\partial^3 \tau}{\partial \alpha^3}\right)_z = -\frac{\cos \alpha}{C_s} \left(\frac{\partial x}{\partial \alpha}\right)_z - \frac{2 \sin \alpha}{C_s} \left(\frac{\partial^2 x}{\partial \alpha^2}\right)_z + \frac{\cos \alpha}{C_s} \left(\frac{\partial^3 x}{\partial \alpha^2}\right)_z \quad .$$

Substituting the values of $\left[\left(\frac{\partial x}{\partial \alpha}\right)\right]_o$ etc, a Taylor series for τ yields:

$$\tau = \tau_o + \tfrac{1}{2} \frac{\cos \alpha_o}{C_s} \cdot \gamma \varepsilon^2 + \frac{1}{6}\left(\frac{\beta \cos \alpha_o}{C_s} - \frac{2\gamma \sin \alpha_o}{C_s} \right) \cdot \varepsilon^3 + O(\varepsilon^4) \qquad \ldots (7)$$

46. Equations (5), (6) and (7) may now be used to express $\left(\frac{\partial x}{\partial \alpha}\right)_z$ and τ in terms of r. In the first place, subtracting $\frac{\cos \alpha}{C_s}$ times equation (5) from equation (7) yields

$$\tau = \tau_o + \frac{r \cos \alpha_o}{C_s} - \tfrac{1}{3} \frac{\gamma \sin \alpha_o}{C_s} \cdot \varepsilon^3 + O(\varepsilon^4) \qquad \ldots (8)$$

Again, from equation (5),

$$\varepsilon = \pm (2r/\gamma)^{\frac{1}{2}} [1 + O(r)] \qquad \ldots (9)$$

where the positive sign belongs to the direct ray, the negative to the 'caustic' ray.

47. Substituting in equations (6) and (8);

$$\left(\frac{\partial x}{\partial \alpha}\right)_z = \pm (2\gamma r)^{\frac{1}{2}} \left[1 + O(r^{\frac{1}{2}})\right] \qquad \ldots (10)$$

$$\tau = \tau_o + \frac{r \cos \alpha_o}{C_s} \mp \frac{1}{3} \frac{\gamma \sin \alpha_o}{C_s} \left(\frac{2r}{\gamma}\right)^{3/2} \left[1 + O(r^{\frac{1}{2}})\right] \qquad \ldots (11)$$

Writing $T = t - \tau_o - \frac{r \cos \alpha_o}{C_s}$ and $\Delta = \frac{1}{3} \frac{\gamma \sin \alpha_o}{C_s} \left(\frac{2r}{\gamma}\right)^{3/2}$, we may substitute from (9), (10) and (11) into equations (4), yielding

$$p_t + p_t' = \sqrt{\frac{\cot \theta_o}{x\sqrt{2\gamma r}}} \left\{ S_o(T + \Delta) \left[1 + O(r^{\frac{1}{2}})\right] + K(\alpha_o)\, S_o(T - \Delta') \left[1 + O(r^{\frac{1}{2}})\right] \right\}$$

But $S_o(T + \Delta) = S_o(T) + \Delta \frac{\partial S_o}{\partial T}(T)$ + higher order terms, and so

$$p_t + p_t' = \sqrt{\frac{\cot \theta_o}{x\sqrt{2\gamma r}}} \left\{ S_o(T) \left[1 + K(\alpha_o)\right] + O(r^{\frac{1}{2}}) \right\} .$$

Now as $r \to 0$ this expression $\to \infty$ unless, and only unless, $K(\alpha_o) = -1$. This, therefore, is the necessary and sufficient condition that we require. Since this result applies to any depth, it amounts to postulating that $K(\alpha) = -1$ for any ray which has passed through a caustic. The sign of p_t is changed; a condensation becomes a rarefaction and vice versa. Physically this is plausible; an elementary ray tube contracts to a point at the caustic and the transport of energy is barred: this is equivalent to the generation of an image source of opposite sign, as in reflection at the vertex of a conical tube.

48. Formally, therefore, we have a complete solution for the transport field beyond a caustic, viz:

$$p = S_o(t - \tau) \sqrt{\left|\frac{\cot \theta}{x\left(\frac{\partial x}{\partial \alpha}\right)}\right|} - S_o(t - \tau') \sqrt{\left|\frac{\cot \theta'}{x\left(\frac{\partial x}{\partial \alpha}\right)'}\right|} \qquad \ldots (12)$$

where the quantities involved are calculated by normal ray-tracing for the 'direct' and 'caustic' rays respectively. It will be rarely the case, however, that this exact calculation is worthwhile. As pointed out earlier, in practical situations the field remote from the caustic is modified by the boundaries of the sea, and may well be a shadow zone. In any case the average field pressure falls off as $r^{-\frac{1}{4}}$ (as is shown by the value of $\frac{\partial x}{\partial a}$ in equation (10)), and there is therefore a focussing effect near the caustic. On both counts the field in the vicinity of the caustic is that of most interest. However in this region equation (12) gives the solution as the difference of two very large quantities - a form unsuitable for numerical calculation.

49. We may, nevertheless, use the results of the preceding analysis to transform equation (12) into an approximate form which will hold in the 'focussing' region near the convergence zone with adequate accuracy. Write $\theta \simeq \theta' \simeq \theta_o$, and (from (10))

$\left|\frac{\partial x}{\partial a}\right| \simeq \left|\frac{\partial x}{\partial a}\right|_{a=0} = \sqrt{2\gamma r}$. Then, with

$t - \tau_o - \frac{r \cos a_o}{c_s} = T$ and $\Delta = \frac{1}{3}\gamma \frac{\sin a_o}{c_s} \left(\frac{2r}{\gamma}\right)^{3/2}$, as before, the total field

$$p \simeq \sqrt{\frac{\cot \theta_o}{x(2\gamma r)^{\frac{1}{2}}}} \left[S_o(T + \Delta) - S_o(T - \Delta) \right] \qquad \ldots (13)$$

50. The justification for neglecting the differences in the amplitudes under the square root sign is as follows. Depending on the nature of the input signal $S_o(t)$ the convergence zone field will show fluctuations in magnitude, and it is only when $S_o(T + \Delta) - S_o(T - \Delta)$ is not small that p will be of practically significant magnitude. But in this situation the small difference between the A_o terms will be of little importance. In other words, equation (13) will be significantly in error only when p is small. But, if the transport field is small, the approximation breaks down in any case, because the dispersive field can no longer be neglected. This argument is perhaps easier to follow in the particular examples that will now be discussed.

THE CW SOURCE

51. For a source $S_o = \exp(i\omega t)$ equation (13) becomes

$$p = \sqrt{\frac{\cot \theta_o}{x(2\gamma r)^{\frac{1}{2}}}} \exp(i\omega T) \cdot 2i \sin(\omega\Delta) \quad . \qquad \ldots (14)$$

The factor i indicates the well-known result that there is a phase change of $\frac{\pi}{2}$ at a caustic of this type.

52. Equation (14) shows that, as a function of range r from the caustic, the amplitude of p is a modulated decaying function of r. The envelope of this is dominated by the $r^{-\frac{1}{4}}$ term; the interference bands are governed by the sin $(\omega\Delta)$ term, since Δ is proportional to $r^{3/2}$ (equation (13)).

53. We may usefully consider the mean square pressure at any point (the conventional 'intensity'). This is

$$I = \langle p^2 \rangle = \frac{\cot \theta_o}{x\sqrt{2\gamma r}} \cdot 4 \sin^2 \left[\frac{\omega \sin \alpha_o \, (2r)^{3/2}}{3C_s \sqrt{\gamma}} \right] \quad \ldots (15)$$

and has the form shown in Figure 5.

54. The transport intensity is zero at the caustic itself (as is true for all types of source). It consists of a series of peaks, of which the first is the largest. The positions of these peaks are given, to sufficient accuracy, by setting $\frac{\omega \sin \alpha_o \, (2r)^{3/2}}{3C_s \gamma^{\frac{1}{2}}} = (2n + 1)\frac{\pi}{2}$, where n is an integer. This gives a series of ranges r_n, the corresponding peak values of I being $\frac{\cot \theta_o}{x\sqrt{2\gamma r_n}}$.

55. The dotted line in Figure 5 represents, schematically, the dispersive field that has so far been neglected. We assume that the frequency is high enough for the asymptotic terms in ω (Section II) to be small compared with the transport term A_o. This implies that the dispersive field is small compared to the peaks of the interference pattern in the transport field. There will also be a dispersive field on the near side of the caustic (a shadow region as far as this part of the wave front is concerned), and this will be continuous across the caustic, as indicated. The effect of this field will be to fill in the troughs of the interference pattern, but to leave the peaks almost unaffected.

56. In addition there are the errors introduced by assuming that $\theta = \theta' = \theta_o$ and $\left(\frac{\partial x}{\partial \alpha}\right) = \left(\frac{\partial x}{\partial \alpha}\right)^1$. The effects of both approximations are shown graphically in Figure 6, in which the two components p_t and p_t' are depicted as vectors in amplitude/phase space. The two solid lines represent the transport field vectors; the small circle represents the contribution of unknown phase arising from the dispersive term. The dotted line represents the resultant. On the right hand side of the figure is given the vector diagram assuming that the two vectors are each equal to the mean value. These sketches illustrate the point made earlier; the error in magnitude is negligible except when the vectors are nearly in anti-phase and the resultant field therefore very small, and therefore unimportant.

57. Returning to Figure 5, a line is drawn showing the 'spherical spreading' prediction of intensity for a unit source; defined here as 20 log x, where x is the horizontal range. The focussing effect near the caustic is clearly shown. The maximum excess of intensity over spherical spreading occurs at the first peak of the interference pattern.

58. To give some feeling for the orders of magnitude involved Figure 5 is based upon a representative situation - a bilinear profile resembling those found in the major oceans. The derivation of these numerical results is given in Appendix I.

59. The essential numerical features are as follows. The source frequency is $3\frac{1}{4}$ kHz. The field point is at the same depth as the source. The caustic appears at a range of 60 km from the source. Interference peaks occur at ranges of $(2n + 1)^{\frac{2}{3}}$ x 100 metres from the caustic. At the first and major peak, 100 metres from the caustic, the excess over spherical spreading is 23 dB, (ignoring attenuation). It seems reasonable to call this the focussing gain. The magnitudes of other peaks follow a - 5 log r law, r being the distance from the caustic.

60. These results are not wildly different from magnitudes observed in practice. They show, however, two features not usually considered. In the first place the convergence zone peak occurs, not at the caustic, but some 100 metres beyond it. Since some experimental investigations of convergence zones have tried to explain discrepancies between predicted and observed ranges of this order of magnitude, this result may be significant.

61. In the second place a fine-grained structure of the field, of scale length of the order of 100 metres or less, is predicted by this theory. Now few experimental investigations have sampled sufficiently closely to reveal a regular structure of this fineness, since at the coarsest a 25 metre sampling interval would be required to delineate the field with any pretence at accuracy. This gives rise to the suspicion that some at least of reported 'fine structure' in convergence zones may be due to inadequate sampling of rapidly varying field.

62. From the point of view of the use of convergence zones for practical purposes such as echo-ranging, detailed prediction of such a fine structure is futile. The effect on the user will inevitably appear as a random statistical fluctuation. This aspect is discussed in Appendix II. Unfortunately, on either a linear or logarithmic scale the statistical distribution of intensity is very skew. However, for operational purposes it is shown in Appendix II that near the peak reasonable simulation may be obtained by assuming that the mean intensity runs at a level 4 dB below the envelope of the peaks, with a standard deviation of 3.8 dB. At greater ranges the mean becomes 3 dB below the peak with standard deviation 3 dB.

HIGH RESOLUTION SONARS

63. For an active sonar there are two paths between sonar and target, of travel times $\tau_o + \Delta$ and $\tau_o - \Delta$ respectively, corresponding to apparent slant ranges of $C\tau_o \pm C\Delta$. The echo may be formed by a pulse going and returning along the same path, or by one following a mixed path. The received signal will therefore consist of a central echo corresponding to range $C\tau_o$ flanked by 'ghosts' at range differences of $\pm C\Delta$. It is appropriate, therefore, to inquire whether a sonar which can resolve these echoes is feasible; the advantage being that the resolved echoes would not be subject to the fluctuations previously discussed.

64. Typical high resolution sonars employ f - m signals (centre frequency f_o, bandwidth B) or a short CW pulse. In the latter case it is convenient to regard the signal as equivalent to one of bandwidth B equal to the inverse of the pulse duration. In both sonars the effective range discrimination is $\frac{C}{2B}$.

65. If the echoes are to be resolved, we must therefore have $\frac{C}{2B} < C\Delta$. But, from equation (14), the m'th null in the interference pattern from the caustic is given by $\omega_o\Delta = m\pi$, or $\Delta = \frac{m}{2f_o}$. The condition for resolution is thus $m > \frac{f_o}{B}$. This may be written as $m > Q$, where Q is the 'Q-factor' of the sonar. Now in practice it is difficult to obtain in an active sonar a value of Q of less than about 3 or 4. It follows that there is little hope of eliminating the interference pattern over the high-focussing region of the convergence zone. In the numerical example quoted even a Q of 3 would produce no improvement out to a range of about 320 metres from the caustic, and a more realistic Q of 7 would correspond to a range from the caustic of 600 m.

66. There is thus no great advantage to be gained in this respect by the use of high-resolution sonars; their other advantages, such as discrimination against reverberation, of course remain.

WIDE-BAND NOISE SOURCE

67. Where passive sonar detection is concerned, or if we can find a suitable broad-band noise source for an active sonar (eg, explosives), the limitations of the previous discussion are considerably relaxed, and it is not difficult to employ bandwidths of an octave or even greater. We should expect such a system to smooth out the interference field, and so to reduce the apparent variability.

68. To illustrate this, consider a unit strength noise source of uniform spectral density $\frac{1}{B}$, with central angular frequency ω_o and bandwidth (expressed in terms of angular frequency) B.

Writing equation (15) in the form

$I = Ar^{-\frac{1}{2}} \sin^2 \omega\Delta$ (where $\Delta \propto r^{3/2}$), the total field becomes

$$\frac{Ar^{-\frac{1}{2}}}{B} \int_{\omega_o-\frac{B}{2}}^{\omega_o+\frac{B}{2}} \sin^2 \omega\Delta \, d\omega$$

$$\text{or } I_N = \tfrac{1}{2}Ar^{-\frac{1}{2}} \left[1 - \cos 2\omega_o\Delta \cdot \frac{\sin (B\Delta)}{B\Delta}\right] . \qquad \ldots (16)$$

69. Since necessarily $B < \omega_o$, the second term in (16) consists of a $\frac{\sin (B\Delta)}{B\Delta}$ envelope modulating the cos $(2\omega_o\Delta)$ sinusoidal variation. If B = 0 we reproduce equation (15).

70. An illustrative plot of equation (16) is given in Figure 7. There are now no nulls in the field (except at the caustic itself), and the effect of the $\frac{\sin (B\Delta)}{B\Delta}$ factor is on the whole to reduce the amplitude of fluctuations as the range increases. The variance about the mean is thus a decreasing function of range.

71. A crude estimate of the standard deviation is derived in Appendix II. The result can be expressed as follows. The mean intensity follows a $-5 \log r$ law, as in the CW situation. The standard deviation at range r from the caustic is approximately

$$\sigma = 1.4\, Q \left(\frac{r_o}{r}\right)^{3/2} \text{ dB}$$

where $Q = \frac{\omega_o}{B} = \frac{f_o}{\delta f}$; and r_o is the range to the first peak.

72. The standard deviation at the first peak is not of great significance; it is more important to consider what happens in the neighbourhood of the first null, for which $\left(\frac{r_o}{r}\right)^{3/2} = \frac{1}{2}$, and therefore $\sigma_{null} = 0.7Q$.

73. Some numerical examples indicate that the foregoing approximations, crude as they are, yield results which look sensible. If we express the Q-factor in terms of octaves it is easy to produce the following:

Bandwidth in octaves	$\frac{1}{3}$	$\frac{1}{2}$	1	∞
equivalent Q	4.33	3.0	1.5	0.5
σ at first peak	6	4.2	2.1	1.0
σ at first null	3	2.1	1.0	0.5

The column headed "∞" arises from the limit

$\lim_{N \to \infty} \frac{1}{2}\left[\frac{2^N + 1}{2^N - 1}\right] = \frac{1}{2}$. It cannot be taken very seriously, except in that it predicts, as we should expect, that for a very wide bandwidth the variance becomes negligible.

74. Comparing the results of this table with the result of the preceeding section - that for a CW pulse the standard deviation is about 3.8 dB near the peak, and 3 dB at greater ranges - we may perhaps draw the useful conclusion that, as far as the high focussing region of the convergence zone is concerned, there will be a useful reduction in variance for bandwidths exceeding one-third octave.

75. For use in operational assessments we might perhaps offer the following rules - albeit with considerable reservations.

a. The mean intensity follows a $-5 \log r$ rule.

b. The standard deviation about this mean may be computed as $1.4\, Q \left(\frac{r_o}{r}\right)^{3/2}$ or 3 dB, whichever is the less.

c. If we are primarily concerned only with sonar detection in the high focussing region of the convergence zone, the standard deviation is 0.7Q or 3.8 dB, whichever is the less.

76. These rules are offered tentatively, on the grounds that they are simple to use, are not unrealistic, and have at least a slender theoretical backing.

EXPLOSIVE SOURCE

77. As an extreme example of a wide-band noise source, we may apply the theory to an exponential source function $\exp(-\mu t) \cdot H(t)$. For a typical 1 lb explosive charge the time constant of the exponential is about 100 micro-seconds, ie, $\mu = 10^4$.

78. It should be made clear at the outset that this simple source is, in fact physically unrealisable. The source pressure has a discontinuous jump at $t = 0$, which no equipment could accept nor the medium sustain. The bandwidth of this source, in fact, is infinite. However, the energy contained in the high frequencies above the cut-off frequency of (in this case) about 1.5 kHz is relatively small, and we may expect the results to be reasonably accurate for a real system as far as energies are concerned, although deductions about peak levels must be carefully considered before acceptance.

79. A direct application of equation (13) to this signal gives immediately

$$p = \sqrt{\frac{\cot \theta_o}{x(2\gamma r)^{\frac{1}{2}}}} \exp(-\mu T) \left[\exp(-\mu\Delta)\, H(T + \Delta) - \exp(\mu\Delta)\, H(T - \Delta)\right] \quad \ldots (17)$$

80. Apart from the amplitude term, the signal consists of a replica of the source signal followed at a time-interval of 2Δ by a phase-reversed replica. The resultant is shown in Figure 8(a). It consists of a positive pressure spike followed by a relatively slowly decaying inversion. It will be noticed that as we approach the caustic (r and Δ both $\to 0$), the amplitude of this initial spike tends to infinity. This physical implausibility is the outcome of our choice of an unrealistic signal; it need cause no concern, however, since both the impulse ($\int p\,dt$) and the energy ($\int p^2\,dt$) in this spike are easily shown to tend to zero. In practice the spike would be rejected by the finite bandwidth of the whole equipment/medium system. Figure 8(b) illustrates schematically what would happen; there would be a finite rate of response, yielding the much more sensible observed signals shown.

81. The quantity of practical interest is the total energy E. From equation (17 it is easy to show that

$$E = 2\mu \int p^2 dT = \frac{2 \cot \theta_o}{x(2\gamma r)^{\frac{1}{2}}} \left[1 - \exp(-2\mu\Delta)\right] . \quad \ldots (18)$$

(The factor 2μ is introduced to normalise the total source energy to unity).

Since $\Delta \propto r^{3/2}$, equation (18) has the form

$$E = \frac{A[1 - \exp(-u)]}{u^{\frac{1}{3}}} \qquad \text{where } u = 2\mu\Delta \quad \ldots (19)$$

82. Its shape is shown in Figure 9 which has been computed for the same profile as for the CW signal. There is a single peak, the position of which can readily be found by setting $\frac{\partial E}{\partial u} = 0$. This yields the transcendental equation $\exp(u) = 1 + 3u$, the solution of which is $u = 1.904$, or $\Delta = 0.95/\mu$.

83. This, for the particular situation considered, gives the peak at 120 metres from the caustic, and a focussing gain of 20 dB (ignoring attenuation). Beyond the peak, since the term $\exp(-2\mu\Lambda) < e^{-2}$, the variation of intensity with range becomes dominated by the $r^{-\frac{1}{2}}$ term of equation (18); as for the CW signal there is a $-5 \log r$ law.

THE VERTICAL FIELD PROFILE NEAR A CAUSTIC

84. It has been shown that there is an interference pattern extending horizontally from each point on the caustic. Since the horizontal range of the caustic itself varies with depth we should expect a similar pattern to be shown if we make a vertical section through the field, ie, keeping the horizontal range x constant. A quantitative development field of this field will now be deduced, using the similar method of analysis to that employed previously.

85. We start with the standard relationship

$$\left(\frac{\partial z}{\partial \alpha}\right)_x \left(\frac{\partial \alpha}{\partial x}\right)_z \left(\frac{\partial x}{\partial z}\right)_\alpha = -1$$

which since $\left(\frac{\partial z}{\partial x}\right)_\alpha = \tan\theta$, the slope of a ray, may be written as

$$\left(\frac{\partial z}{\partial \alpha}\right)_x = -\tan\theta \left(\frac{\partial x}{\partial \alpha}\right)_z \qquad \ldots (20)$$

Since, at the caustic, $\left(\frac{\partial x}{\partial \alpha}\right)_z = 0$, and $\theta = \theta_o \left(\neq \frac{\pi}{2}\right)$, equation (20) shows that $\left(\frac{\partial z}{\partial \alpha}\right)_x = 0$, and thus a Taylor Series expansion is suggested, as before. Writing $z = z_o$, $\left(\frac{\partial^2 z}{\partial \alpha^2}\right)_x = \gamma_1$, $\left(\frac{\partial^3 z}{\partial \alpha^3}\right)_x = \beta_1$, at the caustic; it is easily shown that

$$h = \tfrac{1}{2}\gamma_1 \varepsilon^2 + \frac{1}{6}\beta_1 \varepsilon^3 + \ldots\ldots \qquad \ldots (21)$$

$$\left(\frac{\partial z}{\partial \alpha}\right)_x = \gamma_1 \varepsilon + \tfrac{1}{2}\beta_1 \varepsilon^2 + \ldots\ldots \qquad \ldots (22)$$

where $h = z - z_o$.

For the variation in travel time τ, we use equation (3),

$$\left(\frac{\partial \tau}{\partial \alpha}\right)_x = \frac{\sin\theta}{C}\left(\frac{\partial z}{\partial \alpha}\right)_x \qquad \ldots (3)$$

Also, from the Snell's Law equation

$\frac{\cos\theta}{C} = \frac{\cos\alpha}{C_s}$, it is easy to show that

$$\left(\frac{\partial\theta}{\partial\alpha}\right)_x = \cot\theta \left[\tan\alpha - \frac{1}{C}\left(\frac{\partial C}{\partial z}\right)\left(\frac{\partial z}{\partial\alpha}\right)_x\right] \quad \ldots (23)$$

86. By repeated differentiation of (3), using (23), inserting the values of $\frac{\partial z}{\partial\alpha}$, etc, at the caustic, and substituting in the Taylor series expansion for τ, we can show, in just the same way as previously, that, approximately,

$$\left(\frac{\partial z}{\partial\alpha}\right)_x = \pm\sqrt{2\gamma_1 h}$$

$$t - \tau = T \mp \Delta_1$$

where $T = t - \tau_o - \frac{h\sin\theta_o}{C_o}$

$$\Delta_1 = \frac{\sin\alpha\cot\theta_o}{3C_o}\gamma_1\frac{(2h)^{3/2}}{\gamma_1^{3/2}} ,$$

where the upper sign refers to the direct ray and the lower to the 'caustic ray'.

87. Again, from equation (12), using the relationships just deduced, and making the same approximations as were used in producing equation (13) from equation (12) we have

$$p = \sqrt{\frac{1}{x_o\sqrt{2\gamma_1 h}}}\left[S_o(T - \Delta_1) - S_o(T + \Delta_1)\right] \quad \ldots (24)$$

88. We may now deduce the relationship between equations (13) and (24), starting from the standard differential relationship

$$\frac{\partial}{\partial\alpha}\left[\left(\frac{\partial x}{\partial\alpha}\right)_z\right]_z = \frac{\partial}{\partial\alpha}\left[\left(\frac{\partial x}{\partial\alpha}\right)_z\right]_x + \frac{\partial}{\partial x}\left[\left(\frac{\partial x}{\partial\alpha}\right)_z\right]_\alpha \left(\frac{\partial x}{\partial\alpha}\right)_z$$

whence, from (20), and remembering that $\left(\frac{\partial^2 x}{\partial\alpha^2}\right)_z = \gamma$

$$\gamma = -\frac{\partial}{\partial\alpha}\left(\cot\theta\left(\frac{\partial z}{\partial\alpha}\right)_x\right)_x + \cot\theta\left(\frac{\partial z}{\partial\alpha}\right)_x\frac{\partial}{\partial x}\left[\cot\theta\left(\frac{\partial z}{\partial\alpha}\right)_x\right]_\alpha$$

89. On performing these differentiations, noting that

$\frac{\partial}{\partial x}\left[\left(\frac{\partial z}{\partial a}\right)_x\right]_a = \frac{\partial}{\partial a}\left[\left(\frac{\partial z}{\partial x}\right)_a\right]_x = \frac{\partial}{\partial a}[\tan\theta]_x$, and inserting values at the caustic, it can be shown that

$$\gamma = -\gamma_1 \cot\theta_o \quad . \qquad \ldots (25)$$

90. Equation (25) shows that, for positive γ, γ_1 and hence h are both negative. If we therefore redefine H = − h = depth <u>below</u> the caustic, and

$\gamma_2 = -\gamma_1 = \gamma\tan\theta_o = -\left(\frac{\partial^2 z}{\partial a^2}\right)_x$, it is easily seen that (24) becomes

$$p = \sqrt{\frac{1}{x_o\sqrt{2\gamma_2 H}}}\left[S_o(T_2+\Delta_2) - S_o(T_2-\Delta_2)\right] \qquad \ldots (26)$$

where $\Delta_2 = \frac{\sin\alpha\cot\theta_o}{3C_o}\cdot\frac{(2H)^{3/2}}{\gamma_2^{\frac{1}{2}}}$

$$T_2 = t - \tau_o + \frac{H\sin\theta_o}{C_o} \quad .$$

91. Now equations (13) and (26) are very similar in form, differing only in the constants involved. This difference corresponds essentially to a change in scale of distance, as may be seen from the following considerations. First, for a CW source of frequency ω, Δ and Δ_2 each define a system of interference fringes. For a given fringe $\Delta = \Delta_2$. Then, from equations (13) and (26)

$$\frac{\cot\theta_o \cdot H^{3/2}}{\gamma_2^{\frac{1}{2}}} = \frac{r^{3/2}}{\gamma^{\frac{1}{2}}}$$

or, since $\gamma_2 = \gamma\tan\theta_o$

$$H = r\tan\theta_o \quad . \qquad \ldots (27)$$

It follows that the spacing of the fringes in the vertical plane is reduced by the factor $\tan\theta_o$. In the bilinear example already used $\tan\theta_o \sim 0.1$, so that the first peak is at 10 metres, the second at 21 metres, etc. The intensity at the first peak, from (26), is $\frac{1}{x_o\sqrt{2\gamma_2 H}} = \frac{\cot\theta_o}{x_o\sqrt{2\gamma r}}$, as would be expected.

92. The vertical pattern, therefore, has exactly the same form as in Figure 5, but with the distance scale reduced by the factor $\tan \theta_o$. The same comment will be true for any other type of source, such as the exponential source depicted in Figure 9.

93. There are implications about the use of vertical directivity in this result. From Section IV the horizontal range of the n'th interference fringe is $r_n = (2_n + 1)^{\frac{2}{3}} \times r_o$, where r_o is the distance to the first peak, and therefore at range r_n the vertical distance from the caustic is $H_n = r_n \tan \theta_o$. The vertical spacing of interference fringes at this range is

$$\delta H_n = \tan \theta_o \, \delta r_n = \tan \theta_o \, r_o \frac{2}{3(2_n + 1)^{\frac{1}{3}}} \text{ (putting } \delta_n = 1\text{), or}$$

$$\delta H_n \sim \tfrac{2}{3} \tan \theta_o \frac{r_o^{3/2}}{r_n^{\frac{1}{2}}} \quad .$$

94. In the bilinear example, at a range of 1,000 m from the caustic, since $r_o = 100$ m and $\tan \theta_o \sim 0.1$, $\delta H_n \sim 2$ metres.

95. It is evident that at this range and beyond, the use of a transducer of vertical height approaching 2 metres requires careful consideration by designers.

THE SHAPE OF A CONVERGENCE ZONE

96. The two evaluations of the field already considered may be combined to give a visualisation of the convergence zone field, by deducing the location of the interference fringe pattern with respect to the caustic.

97. In Figure 10, consider a point P_o on the caustic at a point where the slope of the tangential ray, and hence the slope of the caustic, is θ_o. If we consider a particular interference fringe which is at P_1, a horizontal distance r from P_o, then the preceding analysis shows that there will be a point P_2 on the same fringe at a depth $H = r \tan \theta_o$ vertically below P_o. From the geometry of Figure 10 it is apparent that the element P_1P_2 of the fringe has slope θ_o, and this is parallel to the caustic.

98. The closest fringe spacing is therefore in the direction of the normal to the caustic. If d is a distance measured in the direction of the normal, the relationships $r = d \operatorname{cosec} \theta_o$, $H = d \sec \theta_o$, will hold. It is easily seen that the field variation in the direction of the normal to the caustic will be given by the equations:

$$p = \sqrt{\frac{\cos\theta_o}{x_o\sqrt{2\gamma_o d}}}\,[S_o(T_o + \Delta_o) - S_o(T_o - \Delta_o)] \qquad \ldots (28)$$

where $\gamma_o = \gamma \sin\theta_o = \gamma_1 \cos\theta_o$

$$T_o = t - \tau_o + \frac{d}{C_o}$$

$$\Delta_o = \frac{\sin\alpha}{3C_o}\,\mathrm{cosec}\,\theta_o\,\frac{(2d)^{3/2}}{\gamma_o^{\frac{1}{2}}} \quad .$$

99. Equations (28) give, as before, a scaled replica of the fields described by equations (13) and (26).

100. The picture of the field thus assumes a remarkably simple form. The interference fringes form a set of curves parallel to the caustic, the peak intensity following a - 5 log d law from the first peak. From the expression for T_o in equations (28), which represents the 'retarded time' of the mean arrival, we can picture a transmission from the source arriving at the point P_o after travel time τ_o, and then generating a disturbance which travels out normally to the caustic at the local sound speed C_o (ie, the $\frac{d}{C_o}$ term in T).

101. The picture we may form of the 'convergence zone' is thus of a band below the caustic (Figure 11). Some idea of the width of this band may be obtained if we arbitrarily define the remote edge of the convergence zone as that for which the peak intensity is 6 dB below that of the first maximum. Using the - 5 log r law, this gives $r = 17\ r_o$ (and hence $d = 17\ r_o \sin\theta_o$; $H = 17\ r_o \tan\theta_o$). For the bilinear example

r = 1,700 metres, d ~ H ~ 170 metres.

102. A horizontal width of 1,700 metres is not unrealistic for a first convergence zone. It will be noticed that this corresponds to a normal distance from the caustic of only 170 metres. The 'convergence zone' is thus a very thin strip; only the fact that it is nearly horizontal gives a horizontal width as great as 1,700 metres.

NUMERICAL ANALYSIS

103. The exact solution of equation (12), which holds anywhere in the field, requires the computation of grazing angle θ, travel time τ, and horizontal ray spacing $(\frac{\partial x}{\partial \alpha})_z$. These are all quantities which are computed in a normal 'ray-tracing' programme. The only new feature is that crossing rays are added coherently.

104. From the analysis this procedure will be adequate except within a short distance (typically a few hundred metres) from the caustic. As pointed out earlier the solution then becomes the difference between two large but nearly

equal quantities, and the process becomes less and less efficient as the caustic is approached. In this region, therefore, it will be more practical to use the approximation of equation (13) - which will improve the nearer the caustic we approach.

105. For this computation, the only new parameter to be estimated is $\gamma = \left(\frac{\partial^2 x}{\partial \alpha^2}\right)_z$ at the caustic. This presents few difficulties. If the sound speed profile is given in analytically suitable form γ may be computed explicitly (as with the bilinear profile of Appendix I). Otherwise γ may be estimated numerically. The most elementary way is to use the x/α plot of Figure 2; γ is the curvature at the vertex. With modern computer techniques finite difference methods are the obvious choice. In this situation $\frac{\partial x}{\partial \alpha}$ is computed anyway at the point x_n (eg, as $\frac{x_{n+1} - x_{n-1}}{2\delta\alpha}$, where $\delta\alpha$ is the chosen increment of initial grazing angle). Little extra computation is required to evaluate $\frac{\partial^2 x}{\partial \alpha^2}$ (eg, as $\frac{x_{n+1} - 2x_n + x_{n-1}}{(\delta\alpha)^2}$) in the vicinity of the caustic and to interpolate for the value at x_o.

106. In principle, therefore, numerical application of this theory presents few problems.

THE EFFECT OF HORIZONTAL VARIABILITY

107. For convenience and ease of understanding the theory has been developed for a stratified medium. It is, however, not difficult to generalise for a much more general type of medium. A rigorous development will not be given here, but the following arguments are plausible.

108. Assume that the sound speed is specified at every point in the field, and that there is a computational scheme which enables us to evaluate along any ray its slope (θ), travel time (τ), and spreading factor (the A_o term, where $A_o = \sqrt{\left|\frac{1}{x(\frac{\partial \sigma}{\partial n})}\right|}$). Further, let us suppose that this computation has disclosed a caustic, whose position may therefore be taken as known.

109. It is evident that the general result obtained for the stratified medium must still hold, viz: at a field point near the caustic there will be two rays, one 'direct' and the other 'caustic'; the total transport field will always be $A_o S_o(t - \tau) - A'_o S_o(t - \tau')$, where primed quantities refer to the caustic ray. This statement is offerred without rigorous proof, but clearly must be true if an infinite field at the caustic is to be avoided.

110. A solution 'in principle' is therefore to hand, but, as before, is of little practical use in the important region near the caustic; once again we need to find an approximate transition formula. The suggestion is now made that, with some slight modification, the approximation of equation (13) may still be used.

111. We make the usual assumption that the effect of horizontal variability is predominantly in the x-direction, that is, that the ray path will still lie nearly in the same vertical plane throughout. This follows if we assert that the sound speed varies much less rapidly in the horizontal plane than in the vertical.

112. Now equation (13) is based on a Taylor series expansion about a field point on the caustic, and is used essentially to estimate the field only over a relatively short distance (eg, the 170 metres normal distance of the example quoted). As far as the coefficients for expanding x and $\frac{\partial x}{\partial \alpha}$ are concerned, they are computed to the accuracy desired at the origin of the expansion; there is no controversy about their values.

113. The coefficients of the expansion for travel time τ were derived in the case of the stratified medium from the equations $|\text{grad } \tau| = \frac{1}{C}$ and Snell's Law. But both of these equations (provided Snell's Law is given its generalised form) hold for the general case. It can be shown, in fact that in general, if l, m, n, are the direction cosines of ray, the equations

$$\frac{\partial}{\partial \tau}\left(\frac{l}{C}\right) + \frac{1}{C}\frac{\partial C}{\partial x} = 0 \; ; \; \frac{\partial}{\partial \tau}\left(\frac{m}{C}\right) + \frac{1}{C}\frac{\partial C}{\partial y} = 0 \; ;$$

$$\frac{\partial}{\partial \tau}\left(\frac{n}{C}\right) + \frac{1}{C}\frac{\partial C}{\partial z} = 0$$

replace Snell's Law, and the equations $\frac{\partial \tau}{\partial x} = \frac{l}{C}$; $\frac{\partial \tau}{\partial y} = \frac{m}{C}$; $\frac{\partial \tau}{\partial z} = \frac{n}{C}$ hold generally.

114. The resultant expansion of τ can be shown to resolve, with the limitations quoted, into essentially the forms yielding equation (13), provided that θ_o and α are redefined so that they are measured, not from the x-direction, but from the local direction of the contours of C, that is, normal to the direction of grad C. This is equivalent to saying that, at the relevant field point, we treat the medium as a stratified medium, but one in which the stratification is not necessarily horizontal. Very often, in practice, this is a refinement of little quantitative significance.

DISCUSSION

115. It is worth reiterating that the theory presented here is based on a solution of the wave equation which is as valid as, say, a normal mode treatment. Basically, it differs from the latter only in that, while both are in the form of asymptotic solutions, which are most useful only when the leading term is dominant, the impulse solution is an asymptotic series in $\frac{1}{\omega}$, the normal mode treatment in $\frac{1}{\lambda}$. They are therefore complementary, holding, for any given situation, in a high-frequency and a low-frequency domain of validity respectively.

116. There are also the approaches of conventional 'ray theory' and the recent development of 'modified ray theory'. The first of these may be dismissed immediately; the impulse theory contains the whole of 'ray theory' as an approximation, but one in which information on coherence has been lost.

117. The 'modified ray' method and the impulse approach are in many ways similar, and when applicable to the same problem give the same first order asymptotic approximation. The difference lies essentially in the fact that the 'modified ray' technique is based on a steady state (CW) solution of the wave equation, while the impulse technique starts from a δ-function input - an infinite bandwidth. There will therefore be occasions when one technique is more appropriate.

118. In many practical situations such as the convergence zone problem studied here, the impulse technique offers some positive advantages:-

a. The impulse technique gives a solution which is much easier to picture in physical terms. Wave fronts defined by travel time are easier to appreciate than equiphase surfaces (particularly for complex signals), and the 'impulse' rays are well-behaved. Again, for the field in the convergence zone, the mechanism of formation by two rays of opposite phase is readily understandable.

b. The analysis in the impulse technique is simple and uses generally only elementary functions. Compare, for example, the analysis in this study with that for the 'modified ray' approach, which involves finding an asymptotic approximation to an Airy function.

c. The solution for signals of complex form involves an inverse Fourier transform in the CW method; the corresponding problem with the impulse technique is trivial, since the δ-function inverse of a function is just the function itself.

d. The impulse solution is flexible in that it can handle added complexities with comparative ease. For example, it is simple to estimate the effect of a sea-bed which is partially obstructing the formation of the convergence zone: at some limiting range from the caustic the 'direct' ray will be obstructed, leaving only the caustic ray, whose range-dependence law we know.

e. The impulse technique has something in common with the Laplace transform; it has the same knack of picking out a basic feature of the problem which leads directly to a solution. In the convergence zone, for example, the critical feature is the recognition that the rays forming the convergence zone have travelled by almost identical paths, and must therefore be combined coherently.

f. Finally, the close relationship between conventional ray theory and the impulse theory, as far as numerical calculations are concerned, is clearly a great practical advantage.

119. The convergence zone solution presented here has two major features of interest.

120. In the first place, the generality of the solution deserves comment. The form of the solution is not dependent on the details of the sound speed field: to derive it all that is needed is the assumption that a Taylor series expansion exists in the neighbourhood of the caustic. The detailed profile determines only the length scale of the solution. This is an elegant and useful feature.

121. In the second place the theory, for a band-limited signal, predicts a fine-grained variation of intensity with range, the spacing being closer than the spatial resolution of many measurements of oceanic convergence zones.

122. These two results together cast doubt upon some of the attempts that have been made to explain the observed structure of convergence zones by including detail in the sound speed profile: the observations are insufficient and the suggested explanation both inadequate and unnecessary.

123. The theory does, in fact, suggest a useful experimental verification. A long vertical array of suitably spaced hydrophones should reveal the vertical interference pattern from a CW source, and permit a quantitative evaluation. Pending such a crucial test it will not be possible to pass final judgment on the accuracy with which this theory represents reality.

APPENDIX I: CONVERGENCE ZONE FOR A BILINEAR PROFILE

1. The bilinear sound speed profile is shown in Figure 12. The minimum sound speed is denoted by C_V. The source is at height Z_S above the minimum depth, the sound-speed gradient in this region being $-g_1$, so that the sound speed at the source, C_S, has the value $C_V + g_1 Z_S$. Below the minimum is a positive gradient g_2.

2. A typical ray leaves the source at an angle of depression α, crosses the minimum at grazing angle ϕ, turns at a vertex below the minimum and returns to the near surface as shown. We take the field point height Z_F, the sound speed at this point being $C_P = C_V + g_1 Z_F$, and the grazing angle of the ray θ.

From Snell's Law

$$\frac{\cos\theta}{C_P} = \frac{\cos\phi}{C_V} = \frac{\cos\alpha}{C_S} \qquad \ldots (29)$$

and from equation (1) it is easily shown that

$$\left(\frac{\partial\theta}{\partial\alpha}\right)_z = \tan\alpha\cot\theta \; ; \; \left(\frac{\partial\phi}{\partial\alpha}\right)_z = \tan\alpha\cot\phi \qquad \ldots (30)$$

From the normal ray-tracing equations the total range x is given by:-

$$x = 2C_V\left(\frac{1}{g_1} + \frac{1}{g_2}\right)\tan\phi - \frac{C_S}{g_1}\tan\alpha - \frac{C_P}{g_1}\tan\theta \qquad \ldots (31)$$

Differentiating (31) twice with respect to α, using equations (29) and (30), it can be shown that $\left(\frac{\partial x}{\partial\alpha}\right)_z = 0$ gives the relationship

$$2\left(1 + \frac{g_1}{g_2}\right)\operatorname{cosec}\phi_o = \operatorname{cosec}\alpha_o + \operatorname{cosec}\theta_o \qquad \ldots (32)$$

which, with equations (29) determines the values of ϕ, α, and θ at the caustic. It can also be shown that at the caustic the values of

x and $\frac{\partial^2 x}{\partial\alpha^2}$ are then given by:-

$$x_o = \frac{C_S}{g_1}\sec\alpha_o\,(\operatorname{cosec}\alpha_o + \operatorname{cosec}\theta_o)(\sin^2\phi_o - \sin\alpha\sin\theta_o) \qquad \ldots (33)$$

$$\left(\frac{\partial^2 x}{\partial\alpha^2}\right)_o = \frac{C_S}{g_1}\sec\alpha_o\tan^2\alpha_o\,(\operatorname{cosec}\alpha_o + \operatorname{cosec}\theta_o)$$

$$(\operatorname{cosec}^2\alpha_o - \operatorname{cosec}\alpha\operatorname{cosec}\theta_o + \operatorname{cosec}^2\theta_o - \operatorname{cosec}^2\phi_o) \qquad \ldots (34)$$

3. For the particular case where source and field-point are at the same depth, $\alpha = \theta$, and (32), (33), and (34) become, with some manipulation,

$$\left.\begin{aligned} \sin \phi_o &= \left(1 + \frac{g_1}{g_2}\right) \sin \alpha_o \\ x_o &= \frac{2C_S}{g_2} \tan \alpha_o \left(2 + \frac{g_1}{g_2}\right) \\ \gamma &= \left(\frac{\partial^2 x}{\partial \alpha^2}\right)_o = x_o \sec^2 \alpha_o \operatorname{cosec}^2 \phi_o \end{aligned}\right\} \quad \ldots (35)$$

For the particular numerical example, parameter values are:-

$C_S = C_P = 1530 \text{ ms}^{-1}$

$C_V = 1470 \text{ ms}^{-1}$

$Z = 1500 \text{ m}$

$g_1 = 0.04 \text{ s}^{-1}$; $g_2 = 0.02 \text{ s}^{-1}$

With these values,

$\sin \theta_o = \sin \alpha_o = 0.0975 \qquad \alpha_o = \theta_o = 5.6^\circ$

$\sin \phi_o = 0.2925 \qquad \phi_o = 17.0^\circ$

$x_o = 6 \times 10^4 \text{ m}$

$\gamma = 7 \times 10^5 \text{ m}$

Equation (13) then becomes

$$|p| = Pr^{-\frac{1}{4}} [S_o(T + \Delta) - S_o(T - \Delta)]$$

$$\Delta = Qr^{3/2}$$

where $P = 3.78 \times 10^{-4}$

$Q = 7.2 \times 10^{-8}$

CW Source

4. Equation (15), expressed in dB, yields

$$I(dB) = -62.4 + 20 \log |\sin (4.52 \times 10^{-7} f r^{3/2})| - 5 \log r \quad \ldots (36)$$

where f is the frequency in Hertz, and the argument of the sin term is in radians.

5. For a frequency of 3.25 kHz, the first peak occurs when the argument of the sine term = $\frac{\pi}{2}$. This yields r_o = 104 metres, the corresponding value of I being - 72.5 dB. At a range of 6×10^4 m the 'spherical spreading' loss is 95.6, so that the peak focussing gain is 23 dB. (Attenuation has been ignored in this calculation; it would reduce the level by about 6 dB, so that the predicted level would be 17 dB above spherical).

6. A plot of equation (36) is shown in Figure 5.

Explosive Source

7. For the explosive source, with $\mu = 10^4$, equation (18) expressed in dB becomes

$$E(dB) = -65.4 - 5 \log r + 10 \log [1 - \exp(1.44 \times 10^{-3} r^{3/2})] \quad \ldots (37)$$

8. The peak value, for which the argument of the exponential term is 1.904, occurs at range r_o = 120 m, with E = - 75.8, corresponding to a focussing gain (neglecting attenuation) of 19.8 dB. (Once again, absorption has been neglected). Equation (37) is plotted in Figure 9.

9. The similarity of the two peak ranges r_o is to some extent fortuitous; it arises from the fact that the cut-off frequency for the explosive charge (1.5 kHz) is not too far removed from the adopted frequency of 3.25 kHz in the CW situation.

10. It is, in fact, easy to deduce that, for a given environment and a given type of source, the peak range $r_o \propto f^{-\frac{2}{3}}$, while the peak intensity increases with frequency according to a 3.3 log f law.

APPENDIX II: FLUCTUATIONS IN A CONVERGENCE ZONE

1. If we sample fluctuating fields such as those shown in Figures 5 and 7 using range r as the independent sampling variable it is evident that the distribution of intensity, in either linear or logarithmic form, will be extremely skew. One way of approximating such a distribution would be to use a Rayleigh probability function. This would certainly have the right form of skewness, although the actual fit would probably be poor.

2. However, this type of approach has been abandoned in favour of the wildly incorrect choice of a normal Gaussian distribution. The reason for this apparently irrational decision is essentially pragmatic. If we compute a variance about the mean, although this does not necessarily relate to a Gaussian distribution, it does nevertheless have a meaning with respect to the actual distribution. We can at the least use Tschebychev's inequality to establish bounds; even more the variance gives us a yardstick from which to sense the effect of - in this case - increasing the bandwidth. For this purpose, the results are not intended to be used in computation.

3. On the other hand, as a purely practical measure, there are those who require some numerical values, no matter how crude, which can be used in 'broad-brush' studies (such as operational assessments). For such use accuracy in detail is much less important than ease of application combined with an overall 'reasonableness' of the result. It can be argued that such applications will probably involve the combination of a number of statistically ill-described factors, and we could hope that the Central Limit Theorem would smooth out the undesirable features of any one factor. The basic criterion is one of utility, and the addition of variances is an attractively simple technique.

CW Source

4. We may write equation (15) as

$$I = A\, r^{-\frac{1}{2}} \sin^2(\Delta) \qquad \ldots (33)$$

where $\Delta = kr^{3/2}$

To investigate the distribution in the neighbourhood of some range r, consider the behaviour of I over the peak defined by $n\pi \leq \Delta \leq \overline{n+1}\,\pi$. For our crude approximation we shall neglect the variation of the $r^{-\frac{1}{2}}$ term over the range and also use Δ as the independent variable instead of r.

Thus $\overline{I} \simeq A\, r^{-\frac{1}{2}}\, \overline{\sin^2 \Delta} \sim \frac{Ar^{-\frac{1}{2}}}{2}$

and $\overline{I^2} \sim A^2 r^{-1}\, \overline{\sin^4 \Delta} \sim \frac{3}{8} A^2 r^{-1}$

whence $\sigma^2 = \overline{I^2} - (\overline{I})^2 = \frac{1}{2}(\overline{I})^2$

This is in linear terms. If we write

$u = 10 \log_{10} I = 4.34 \log_e I$, then $\delta u \simeq 4.34 \frac{\delta I}{I}$, which (provided the

variation is not too great) can be used to deduce $\sigma(\text{dB}) = \frac{4.34}{\sqrt{2}} \sim 3$. The mean, $\overline{I}$, is - 3 dB from the peak value.

5. This result, that the mean level is 3 dB below the peak level, with a standard deviation of 3 dB, will be not unreasonable at relatively large distances from the caustic. However, major interest will, of course, concentrate on the region near the caustic, and for this reason the first peak has been treated somewhat differently. The distribution of $10 \log_{10} I$ as a function of range has been computed over the first peak (ie, to range r_o). The results, showing the proportion of range for which I exceeds a given level (measured in dB from the peak value) is given in the Table.

Distribution of I over the first peak

I (dB from peak)	0	-1	-2	-3	-4	-5	-6	-7	-8
Proportion of range for which intensity > I	0	0.28	0.39	0.47	0.52	0.57	0.62	0.66	0.69

6. The "50%" point is about - 4 dB, and about 0.68% lie within the range 0 to - 7.7 dB; the "standard deviation" is therefore taken as half this, ie, - 3.3 dB. It is these figures that are quoted in Section IV.

Band-Limited Source

7. The field from this source is discussed in Section VI.

8. It is clear from equation (16) and Figure 7 that there is a variation about a mean level following a - 5 log r law. This variation has a relatively rapid component arising from the cos $2\omega_o\Delta$ term of equation (16) together with a fluctuating, but on the whole decreasing, envelope modulation due to the $\frac{\sin B\Delta}{B\Delta}$ factor. The greater the bandwidth is, the smaller the amplitude of the fluctuations becomes, and the more reasonable it seems to use the Gaussian approximation.

9. We start with equation (16)

$$I = \tfrac{1}{2} A r^{-\frac{1}{2}} \left[1 - \cos 2\omega_o\Delta \frac{\sin (B\Delta)}{B\Delta}\right]$$

and, as before, treat the $r^{-\frac{1}{2}}$ and $B\Delta$ terms as constant, and use Δ as the independent variable.

10. Averaging over a cycle of the $B\Delta$ term, we have $\overline{I} = \frac{1}{2} A r^{-\frac{1}{2}}$, and thus

$$I - \bar{I} = -\frac{\bar{I} \cos 2\omega_o \Delta \sin (B\Delta)}{B\Delta}$$

whence $\sigma^2 = \overline{(I - \bar{I})^2} = \frac{\bar{I}^2}{B^2\Delta^2} \cdot \frac{1}{4}$

and, using as before the approximate relationship

$$\sigma\,(\mathrm{dB}) = 4.34\,\frac{\sigma}{\bar{I}}$$

we have $\sigma\,(\mathrm{dB}) = \frac{2.17}{B\Delta}$

But, if $\Delta = kr^{3/2}$, we have, for the first peak

$$\omega_o \Delta_o = \omega_o\, kr_o^{3/2} = \frac{\pi}{2}$$

whence $\Delta = \frac{\pi}{2\omega_o} \cdot \left(\frac{r}{r_o}\right)^{3/2}$

and thus

$$\sigma(\mathrm{dB}) = 1.4 \left(\frac{r_o}{r}\right)^{3/2} \cdot \frac{\omega_o}{B} = 1.4Q \left(\frac{r_o}{r}\right)^{3/2} .$$

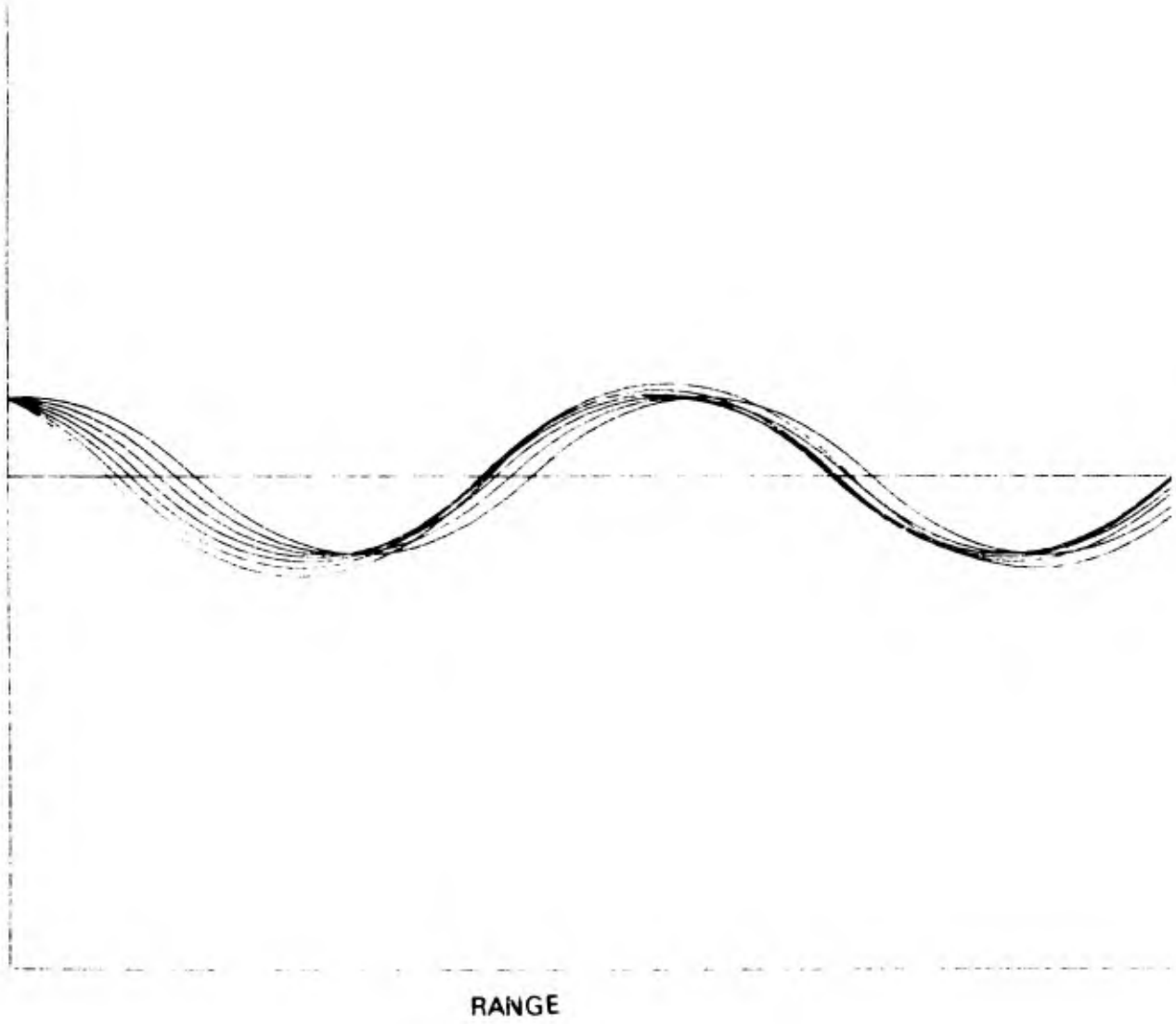

THE FORMATION OF A CONVERGENCE ZONE.
FIGURE 1.

FIG. 1

FIG . 2

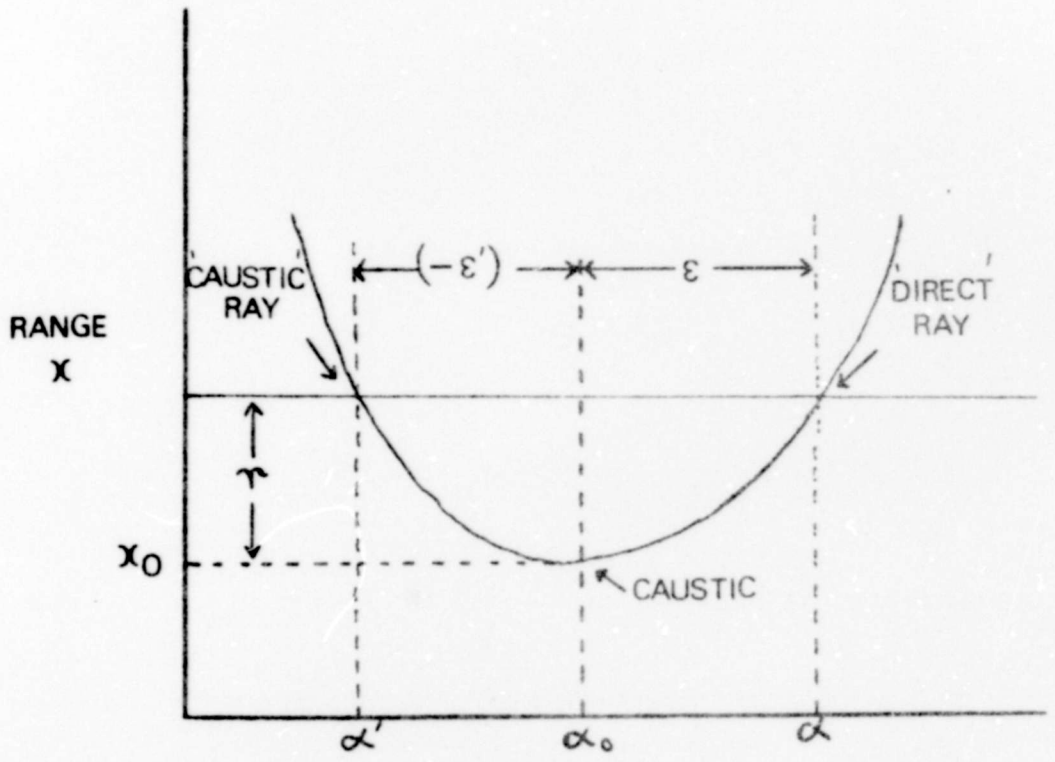

FIGURE 2. RANGE VS INITIAL GRAZING ANGLE.

SPACING 1500 METRES (1 SECOND)

FIG.3

FIGURE 3. WAVE FRONTS IN CONVERGENCE ZONE

FIG. 4

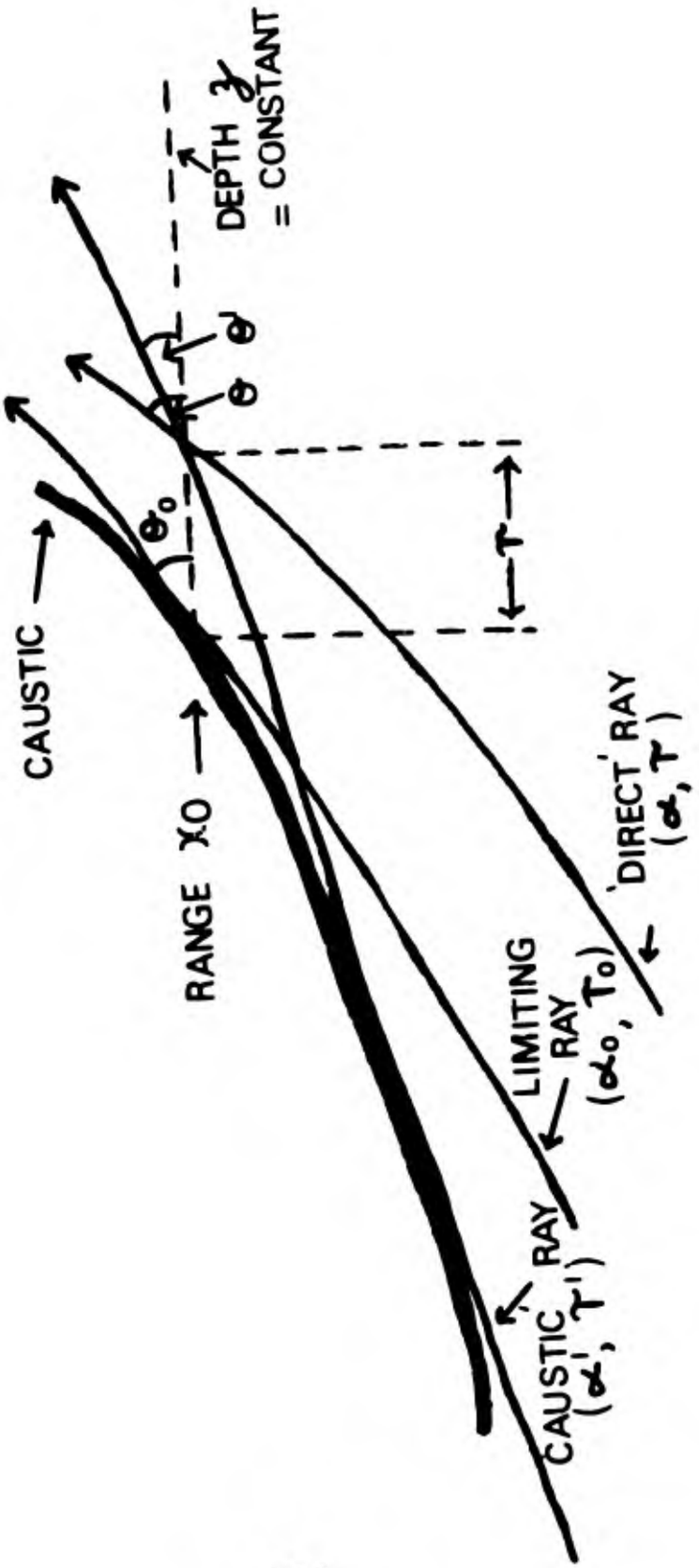

FIG. 4. THE RAYS FORMING A CAUSTIC

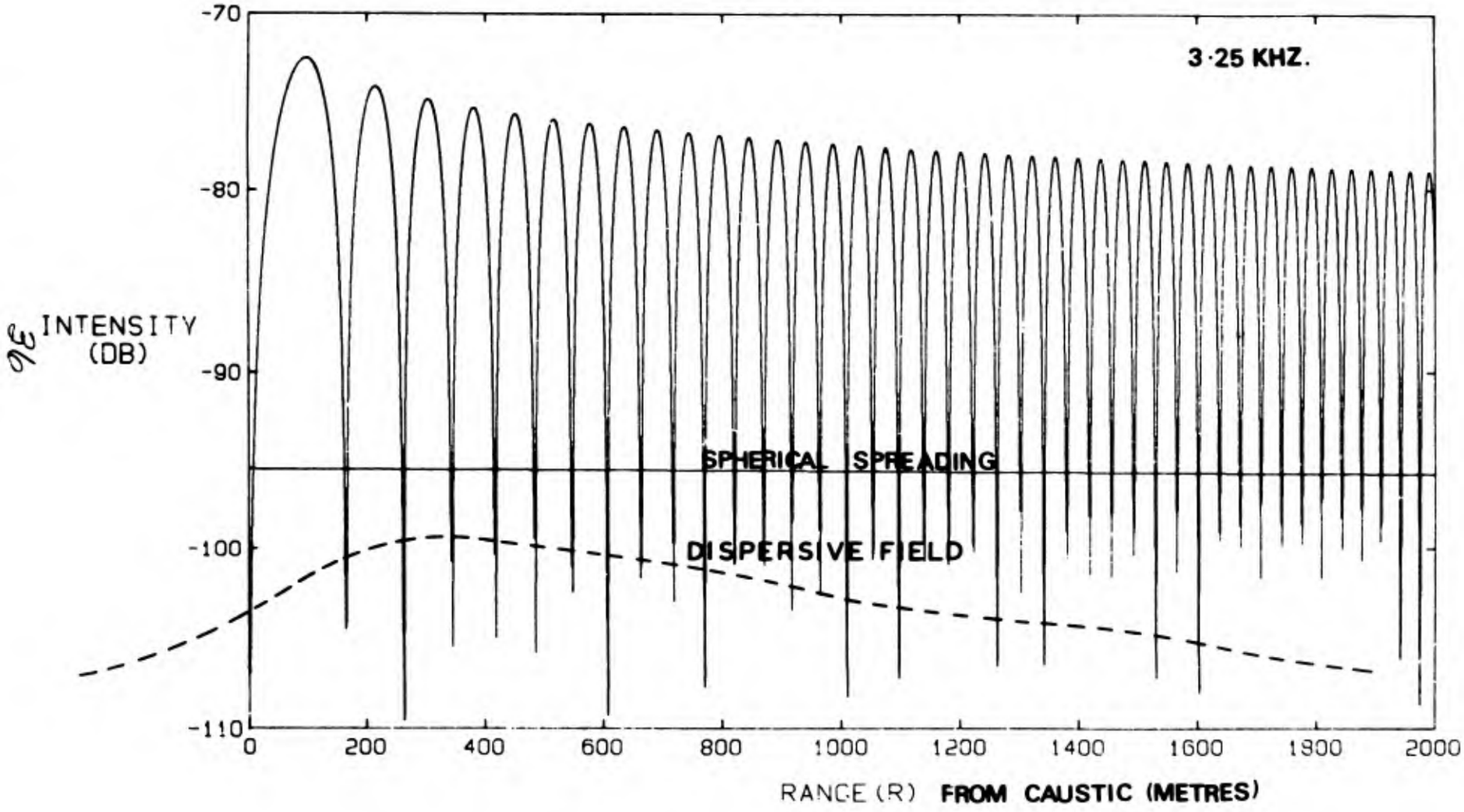

FIGURE 5. INTENSITY VS RANGE – C W SOURCE.

FIG. 5

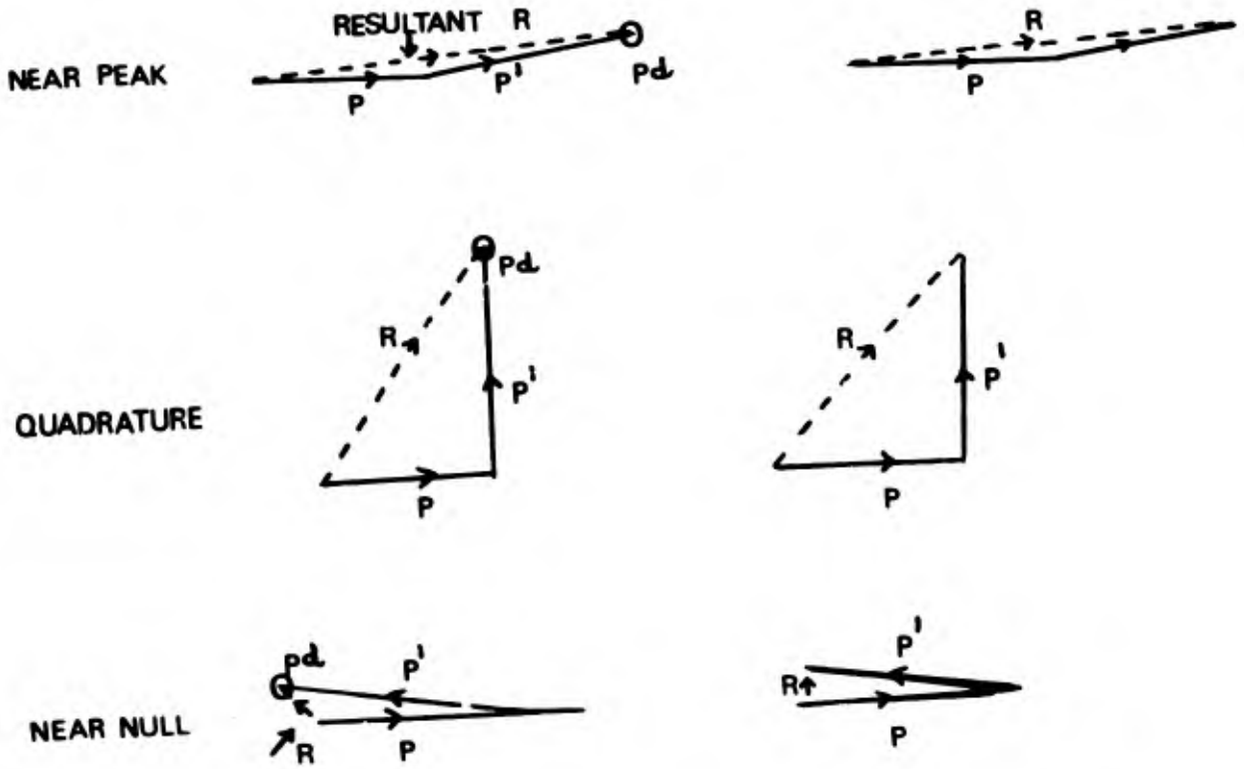

FIG. 6.

FIGURE 6. VECTOR REPRESENTATION OF CW FIELD

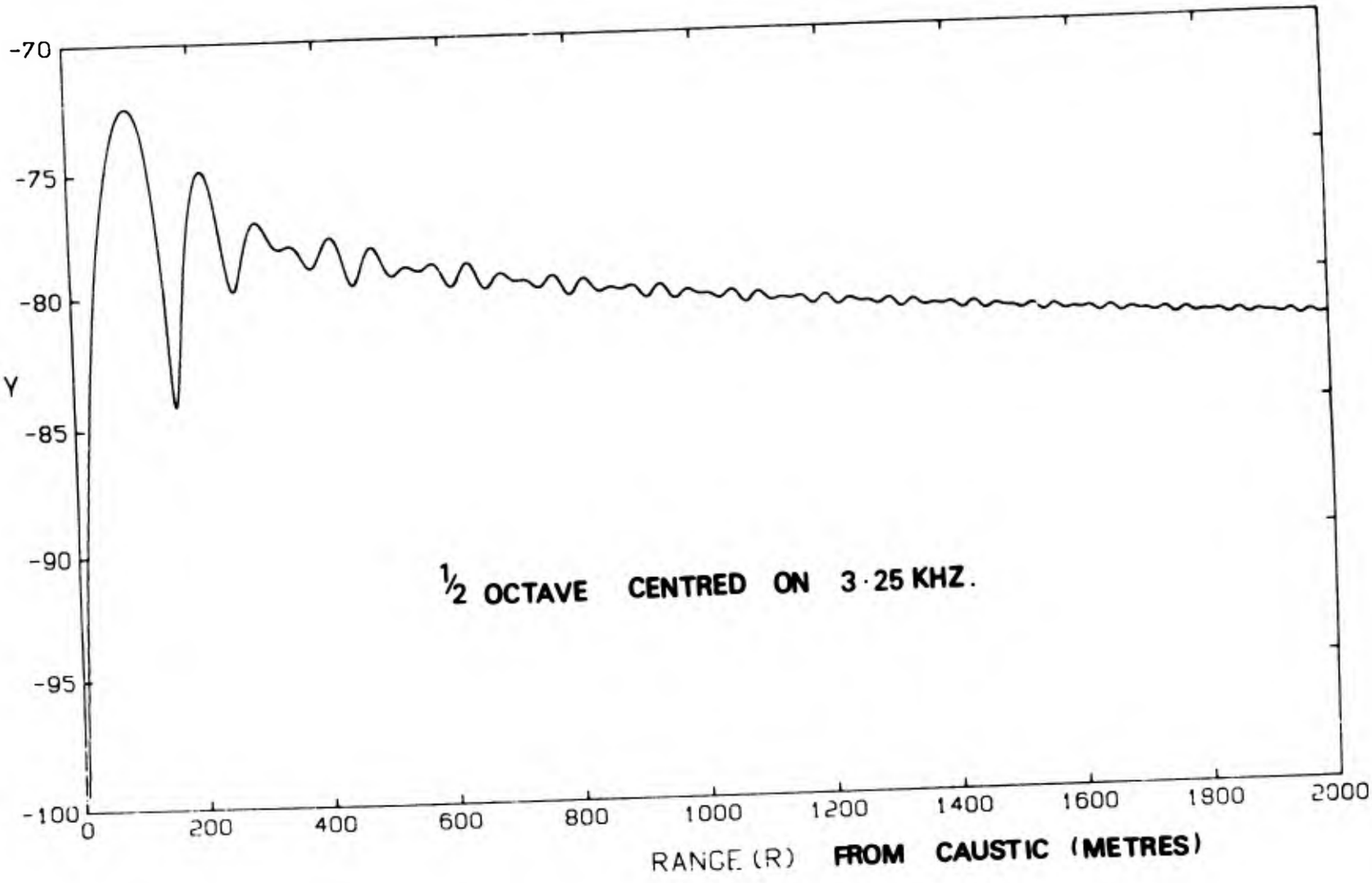

38

FIG. 7

FIGURE 7 INTENSITY VS RANGE - BAND LIMITED SOURCE.

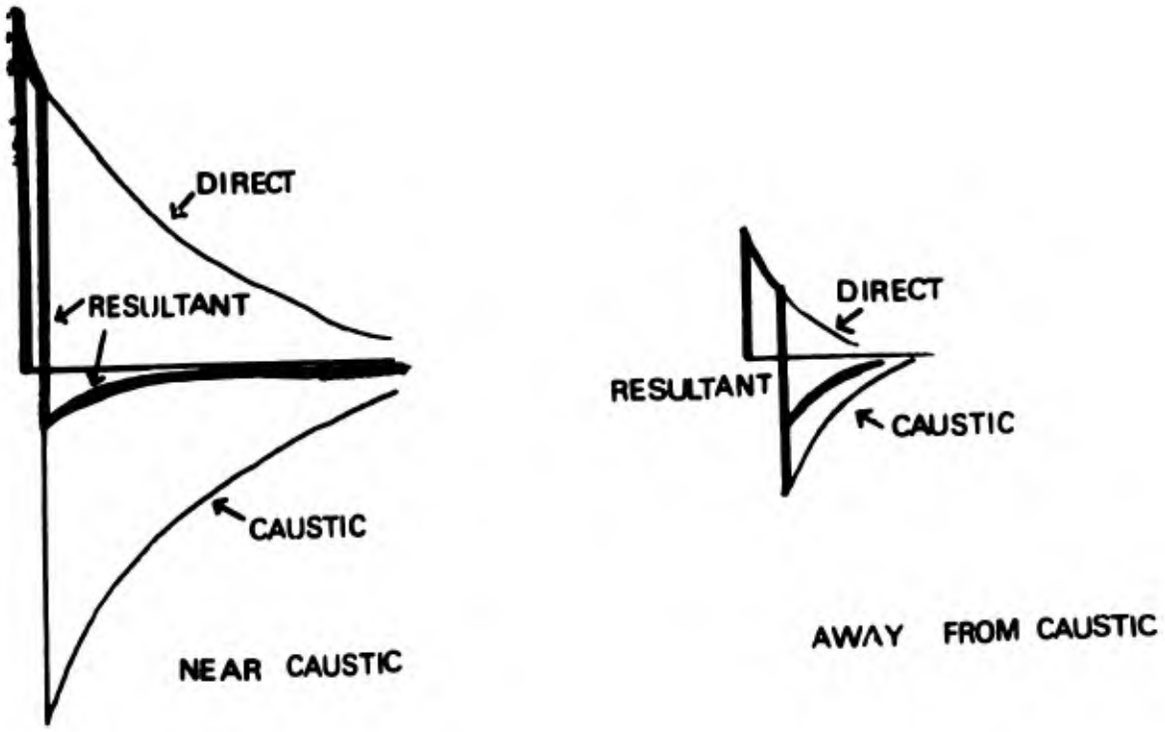

(A) INFINITE BANDWIDTH

(B) HIGH FREQUENCY CUT-OFF (FINITE RESPONSE TIME)

FIGURE 8. SIGNAL FROM EXPLOSIVE SOURCE.

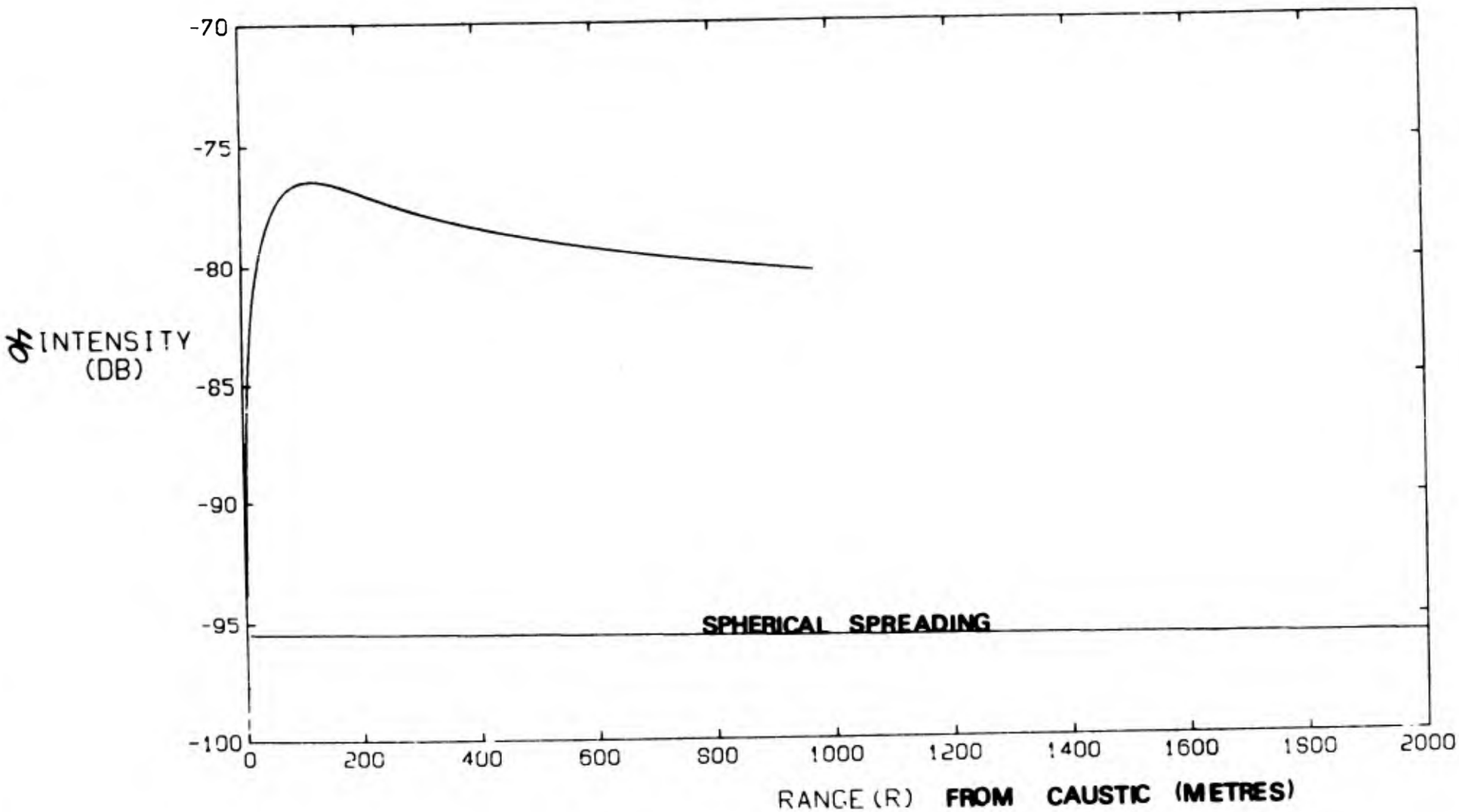

FIG. 9

FIGURE 9. INTENSITY VS RANGE EXPLOSIVE SOURCE

$$H = \tau \tan \theta_0$$

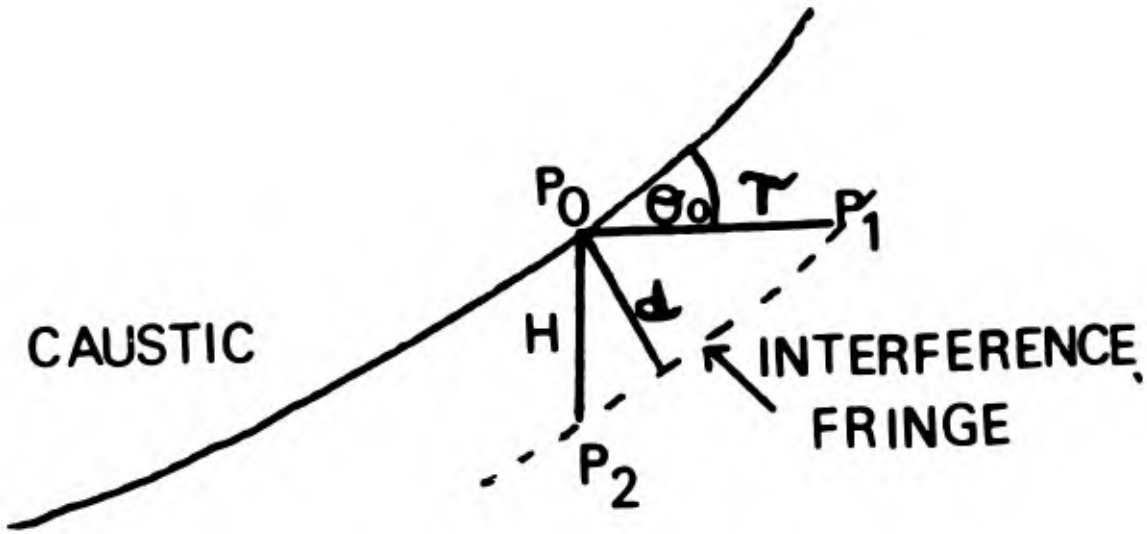

FIG.IO. RELATIONSHIP BETWEEN VERTICAL AND HORIZONTAL FINE STRUCTURES

FIG.IO

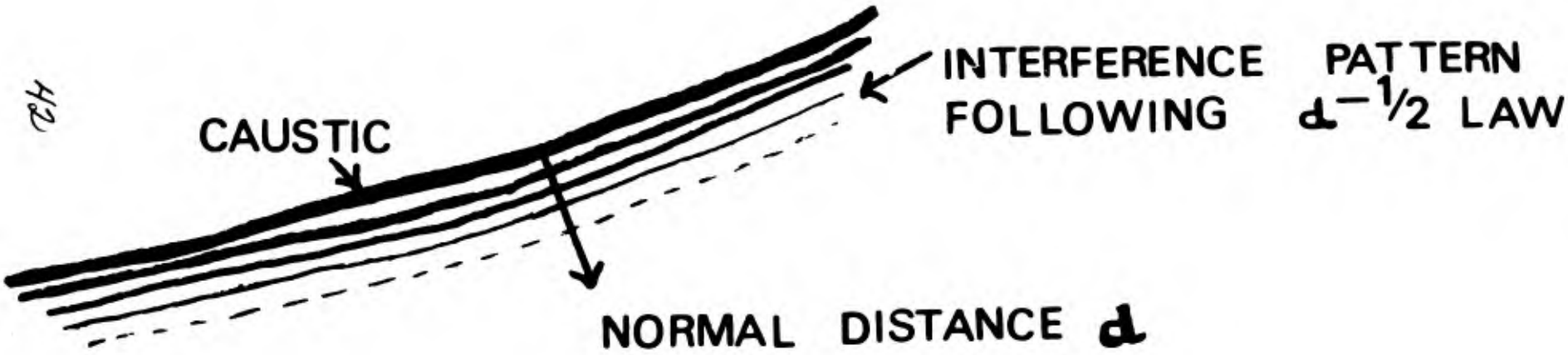

FIG. 11. THE SHAPE OF A CONVERGENCE ZONE

FIG. 11.

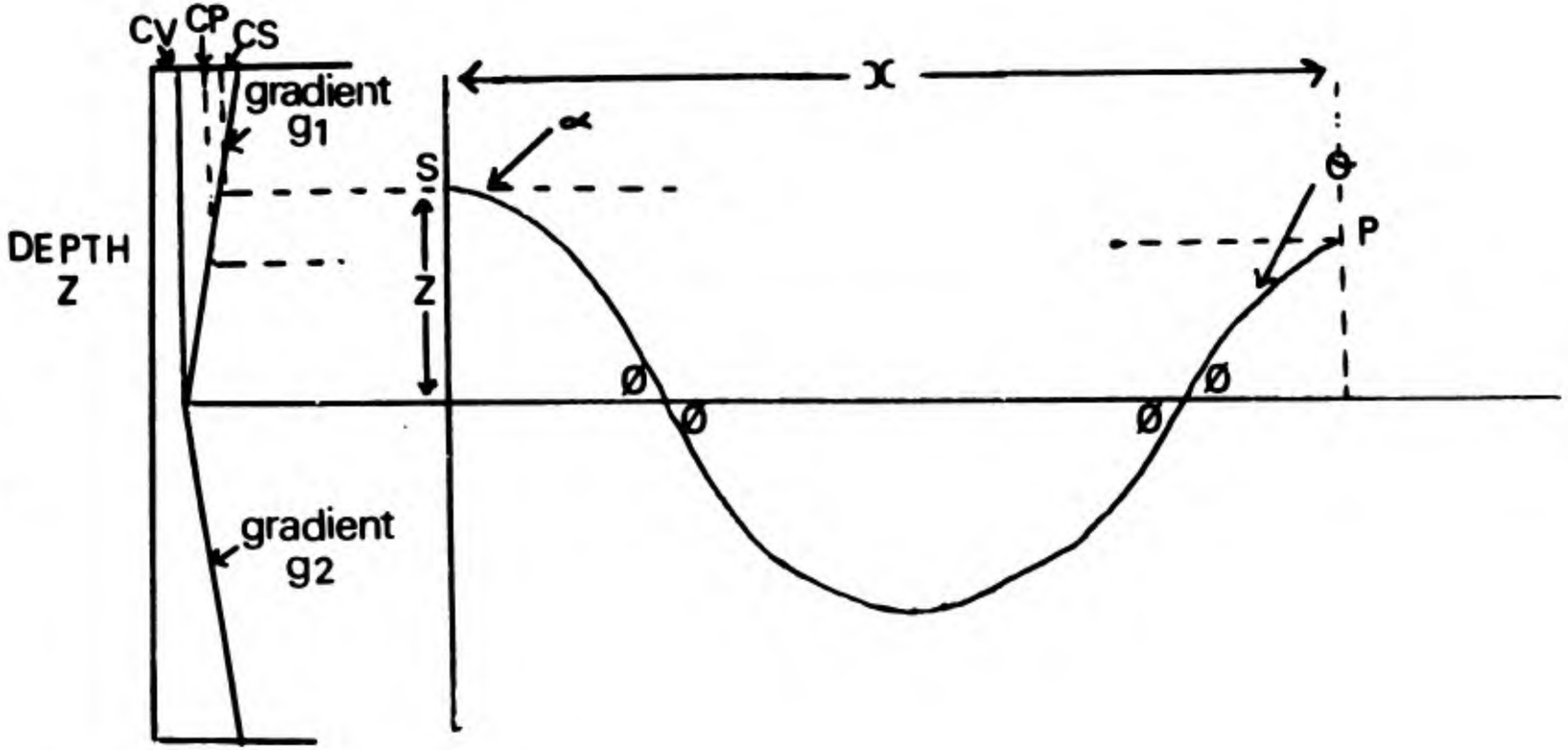

FIG.12

FIGURE 12 RAY PATH FOR BILINEAR PROFILE